U.PORTO
FEUP FACULDADE DE ENGENHARIA
UNIVERSIDADE DO PORTO
INSTITUTO DE CIÊNCIAS BIOMÉDICAS ABEL SALAZAR
UNIVERSIDADE DO PORTO

ULTRASTRUCTURAL FEATURES OF CALICIVIRUS INFECTION

VÍTOR DANIEL GONÇALVES CARNEIRO

Dissertação de Mestrado em Bioengenharia

2013

VÍTOR DANIEL GONÇALVES CARNEIRO

ULTRASTRUCTURAL FEATURES OF CALICIVIRUS INFECTION

Dissertação de Candidatura ao Grau de Mestre em Bioengenharia – Biotecnologia Molecular submetida ao Instituto de Ciências Biomédicas Abel Salazar

Orientador: Doutor David Bhella

Categoria: Professor Honorário

Afiliação: Universidade de Glasgow

Co-orientador: Doutora Maria São José Alexandre

Categoria: Professor Catedrático

Afiliação: Faculdade de Farmácia da Universidade do Porto

ULTRASTRUCTURAL FEATURES OF CALICIVIRUS INFECTION

GONÇALVES C., DANIEL[1,2,3]

1 – Abel Salazar Biomedical Sciences Institute
2 – Faculty of Engineering of the University of Porto
3 – Medical Research Council University of Glasgow Centre for Virus Research
4 – Faculty of Pharmacy of the University of Porto

This dissertation was developed under supervision of

Dr. David Bhella[3]

and co-supervision of

Professor Maria São José Alexandre[4]

The author

(Vítor Daniel Gonçalves Carneiro)

The co-supervisor

(Professor Maria São José Alexandre)

PREFACE

This thesis is organized into four chapters: a general introduction and three chapters where results obtained are presented and discussed. The general introduction gives an overview of the molecular biology of caliciviruses, in particular, feline calicivirus, with a brief description of its structure and relevant host-cell interactions. This section also reviews electron microscopy and three-dimensional reconstruction techniques. Regarding the results, chapter two analyzes the structure of recombinant Sapporo virus-like particles and compares different three-dimensional reconstructions. Chapter three concerns the conformational changes that feline calicivirus undergoes in low pH environment. In the last chapter, structural features of the feline calicivirus RNA replication complexes in the context of the whole cell are discussed.

The work herein described is the product of a six month internship carried out by the author at the Medical Research Council University of Glasgow Centre for Virus Research, in Glasgow, Scotland, United Kingdom, under the supervision of Dr. David Bhella.

Nothing in life is to be feared, it is only
to be understood.
Now is the time to understand more,
so we can fear less.

Marie Skłodowska-Curie

ACKNOWLEDGEMENTS

During the elaboration of this dissertation, several people contributed to the development of the work. Herein, I humbly acknowledge all the inspiring people I worked with and helped me to complete this project.

I would like to acknowledge, most of all, my supervisor **Dr. David Bhella**, who welcomed me in his group, and taught me everything I know about virology and microscopy. His dedicated patience to teach science and his passion for virology will always inspire me. I also would like to thank the rest of the lab group: **Swetha**, **Richard**, **Saskia**, **Ivan**, **Rebecca**, **Marion**, and in particular **Colin**, who accompanied me throughout the entire project and always showed me the silver lining every time I had a bad result. **Dr. Frazer Rixon**, who helped me with the resin embedding section, and **Professor Brian Willett**, who welcomed me in his lab and help me with tissue culture and virus propagation, and the rest of his lab group. A special thank you goes to **Dr. Ayman Samman** for all the teaching and never-ending patience answering all my questions. For all the guidance, support and friendship, **Dr. Filipe Nunes**, and **Professor Massimo Palmarini**, director of the Centre for Virus Research in Glasgow, who believed in me and offered me this opportunity to work in this amazing institute.

I would like to acknowledge **Professor Maria São José Alexandre**, my co-supervisor in Porto, for all the support, guidance and faith in my work.

I acknowledge the Medical Research Council University of Glasgow Centre for Virus Research, which funded this project and the ERASMUS mobility programme, an integral part of the Lifelong Learning Programme of the European Commission who supported me during my stay in the UK.

Moreover, a special thank you goes to **Pranav**, **Becca**, **António**, **Matt**, **Eva**, **Joanna**, and **Jaclyn** for all the amazing times during my stay in Glasgow, and to my closest friends in Porto: **Margarete**, **Rita**, **Iúri**, **Cláudia** and **Isa**, who showed me that friendship sees no boundaries, no distance. Above all, thank you, **Andreia**, for being my buddy while exploring the UK and the British culture, and for making this experience unforgettable. To a lifetime friendship.

Finally, I would like to acknowledge my **parents**, especially my **mother**, for being a role model of effort, dedication, tenderness and love. And my **sister**, who is the reason why I never give up.

LIST OF ABBREVIATIONS

ATP	Adenosine triphosphate
CCD	Charged-coupled device
CCF	Cross-correlation function
CCID50	Cell culture infectious dose 50%
CRFK	Crandell-Reese feline kidney
CryoEM	Cryo-electron microscopy
CTF	Contrast transfer function
DMEM	Dubecco's modified Eagle's medium
DNA	Deoxyribunocleic acid
EBHSV	European brown hare syndrome virus
eIF3	Eukaryotic translation ignition factor 3
eIF4E	Eukaryotic translation ignition factor 4E
EM	Electron microscopy
ER	endoplasmic reticulum
FCV	Feline calicivirus
FEA	Feline embryonic fibroblasts
fJAM-A	Feline junction adhesion molecule A
GTP	Guanosine triphosphate
LC	Leader of the capsid protein
MNV	Murine norovirus
MOI	Multiplicity of infection
NTA	N-terminal arm
NTPase	Nucleoside triphosphatase
ORF	Open reading frame
P	Protruding
PBS	Phosphate buffered saline
PCR	Polymerase chain reaction
PEC	Porcine enteric calicivirus
PEG	Polyethylene glycol
Pro-pol	Proteinase-polymerase
PTB	Polypyrimidine tract-binding
RdRp	RNA-dependent RNA polymerase
RHDV	Rabbit haemorrhagic disease virus
RNA	Ribonucleic acid
RT-PCR	Reverse transcription-polymerase chain reaction
rVP1	Recombinant viral protein 1

S	Shell
SMSL	San Miguel sea lion virus
SV	Sapporo virus
SVLPs	Sapovirus –like particles
TEM	Transmission electron microscope
VESV	Vesicular exanthema of swine virus
VLPs	Viral-like particles
VP1	Viral protein 1
VP2	Viral protein 2
VPg	Viral protein linked to the genome
VS-FCV	Virulent strain of feline calicivirus

CONTENTS

TABLE OF FIGURES

ABSTRACT

The *Caliciviridae* is a family of small, nonenveloped, positive-stranded RNA viruses that cause a wide range of diseases in their hosts, including acute gastroenteritis in humans, and respiratory illness, systemic and haemorrhagic diseases in animals. This family is divided into five genera: *Lagovirus*, *Nebovirus*, *Norovirus*, *Sapovirus*, and *Vesivirus*. *Norovirus* and *Sapovirus* are the only genera to contain species that infect humans, and together are the worldwide leading cause of acute gastroenteritis. The study of calicivirus infection, however, has been hindered by the lack of an efficient *in vitro* culture system. Still, some species can be propagated in cell culture, including *Feline calicivirus* (FCV), which has been used for several decades as a tractable model to help to understand the infection mechanisms of caliciviruses. FCV belongs to the *Vesivirus* genus of *Caliciviridae* and is of major importance in small animal veterinary medicine; generally causing oral and upper respiratory tract disease in felids, although recently virulent strains have emerged that cause systemic disease with a high mortality rate. In recent years, its physiological receptor – feline junction adhesion molecule – was identified, enabling studies that elucidate the attachment and mechanism of entry of related viruses. Such studies may contribute to the development of a culture system for human caliciviruses, inasmuch as the attachment and entry step is the block in efficient human calicivirus growth in cell culture. Herein, we exploit cryo-electron microscopy and three-dimensional image reconstruction techniques to better assess structural insights of calicivirus infection.

In order to evalute three-dimensional image reconstuction techniques, we compared recombinant Sapporo virus-like particles reconstructions (derived from a human sapovirus that belongs to the *Sapovirus* genus) with reconstructions of related caliciviruses. These reconstrcutions were calculated using different three-dimensional image reconstruction software, namely EMAN and BSFOT in combination with PFT2/EM3DR. Furthermore, we exploited cryo-electron microscopy and three-dimensional reconstruction to understand FCV cell entry, in particular, the effect of low pH environment in the endosome. We observed that FCV undergoes a dramatic conformational change at low pH that might relate to viral genome penetration. We also assessed FCV RNA replication in Feline Embryonic fibroblasts, which has been shown to occur in FCV-induced membrane-bound vesicles. We observed that such vesicles are related to the endoplasmic reticulum of the host cell and possess connecting regions between each vesicle.

To conclude, the data presented here shows how FCV is able to interact with different structures of the host cell in order to sucessfully infect and replicate, highlighting the importance of low pH environment in endosomes and endoplasmic reticulum (ER) deformation in the early stages of FCV infection.

RESUMO

Caliciviridae é uma família de vírus de RNA de polaridade positiva e sem invólucro, sendo responsáveis por uma vasta gama de doenças do epitélio nos seus hospedeiros, incluindo gastroenterite aguda em humanos, e doenças respiratórias, hemorrágicas e sistémicas em animais. Esta família contém cinco géneros: *Lagovirus*, *Nebovirus*, *Norovirus*, *Sapovirus*, e *Vesivirus*. Os géneros *Norovirus* e *Sapovirus* são os únicos que contêm espécies que infetam seres humanos, sendo a principal causa de gastroenterite aguda. Contudo, o estudo da infeção por calicivirus tem sido dificultada pela falta de sistemas eficientes de cultura *in vitro*. Ainda assim, algumas espécies podem ser propagadas em cultura de tecidos, incluindo o calicivirus felino, o qual tem sido utilizado como um modelo para o estudo do mecanismo de infecção de calicivirus. Este vírus pertence ao género *Vesivirus* da família *Caliciviridae* e assume uma grande importância na veterinária de animais de pequeno porte; causa geralmente doenças orais e do tracto respiratório superior em felídeos, embora outras estirpes mais virulentas tenham emergido recentemente causando uma síndrome sistémica com elevada taxa de mortalidade. Recentemente, o recetor fisiológico do calicivirus felino foi identificado – a molécula de adesão das *tight-junctions* – possibilitando estudos que investiguem o mecanismo de adsorção e entrada do vírus na célula do hospedeiro. Estes estudos podem contribuir para o desenvolvimento da cultura de calicivirus humanos, uma vez que a adsorção e entrada do vírus da célula foram identificadas como o passo que impossibilita a propagação de calicivirus humanos em cultura. Neste documento, técnicas de crio-microscopia eletrónica e reconstrução tri-dimensional de imagens são exploradas para estudar as interações estruturais na infeção por calicivirus.

Para avaliar diferentes técnicas tri-dimensionais de reconstrução de imagem, reconstruções de Sapporo “virus-like particles” recombinantes (geradas a partir de um sapovirus humano pertencente ao género *Sapovirus*) foram comparadas com recontruções de outros calicivirus. Estas reconstruções foram calculadas usando diferente *software* de reconstrução tri-dimensional, nomeadamente o programa EMAN e o BSFOT em combinação com PT2/EM3DR. A entrada celular do calicivirus felino também é estudada recorrendo a técnicas de microscopia, em particular o efeito do pH ácido dos endossomas na cápside viral. Foi observado que o calicivirus felino sofre uma dramática mudança conformacional a baixo pH que poderá estar relacionado com a penetração do genoma no citoplasma. Por último, reportamos um estudo sobre a replicação do calicivirus

felino em fibroblastos embriónicos de origem felina, que ocorre em vesículas membranares induzidas pelo virus. Os resultados deste estudo mostram que a formação de vesículas está relacionada com o retículo endoplasmático das células do hospedeiro e possuem regiões de comunicação entre elas.

Em suma, os resultados apresentados aqui mostram que o FCV é capaz de interagir com diferentes estruturas da célula, realçando a importância do baixo pH nos endossomas e a reorganização do retículo endoplasmático em estádios iniciais da infeção.

CHAPTER 1

General Introduction

1. Caliciviridae

The *Caliciviridae* are a family of non-enveloped, positive-stranded RNA viruses that infect a wide range of animals causing diseases, such as gastroenteritis and respiratory illness (Clarke and Lambden 1997). Members of this family, commonly designated as caliciviruses, belong to Class IV of the Baltimore Scheme for animal virus genome classification (Baltimore 1971). The name of the family derives from the latin word for cup – *calyx* – in reference to the morphology of these viruses under electron microscopy (EM): the invaginations found in calicivirus capsids are often described as cup-like depressions (Zwillenberg and Burki 1966).

Historical Overview

For the past 80 years, calicivirus infections have been reported in a broad range of animals, mainly mammals but sometimes in birds and reptiles too. The vesicular exanthema of swine virus (VESV) was the first calicivirus to be identified and was found in pigs in California in 1932 (Hopkins 1958). These swine calicivirus infections had their source in some calicivirus species of marine mammals, in particular the San Miguel sea lion virus (SMSV) that were isolated in the northern Pacific Ocean (Smith, Skilling et al. 1998, Etherington, Ring et al. 2006). Feline calicivirus (FCV) was first isolated in 1957 from feline kidney cells (Fastier 1957). Fastier was trying to induce an infection of feline panleukopenia virus, when this new virus appeared to induce a different phenotype in cell culture. First, FCV was designated as kidney cell-degenerating virus and later Feline picornavirus, since at that time caliciviruses were considered a genera of *Picornaviridae* (Burki 1965). Due to the subsequently discovered differences between caliciviruses and picornaviruses, the *Caliciviridae* family was created in 1976 (Fenner 1976). In China, 1984, a calicivirus was discovered in rabbits, which caused a fatal disease. This was designated rabbit haemorrhagic disease virus (RHDV) and was later identified in other countries throughtout the world (SJ, HP et al. 1984, Abrantes, van der Loo et al. 2012).

Only two caliciviruses are known to infect humans: human noroviruses and sapoviruses. Human norovirus was first identified in an acute gastroenteritis outbreak in Norwalk, Ohio, in 1968 (Adler and Zickl 1969). Since then, human norovirus has been described in numerous outbreaks in cruise ships and hotels as well as in instituitions such as schools, hospitals and care-homes. Sapporo virus was first isolated during a

gastroenteritis outbreak in an orphanage in Sapporo, Japan, in 1977. Human sapovirus also has a worldwide destribution and is frequently associated with outbreaks of infantile gastroenteritis in Asia. (Chiba, Nakata et al. 2000) Human noroviruses and sapoviruses are the worldwide leading cause of acute gastroenteritis in human (Patel, Widdowson et al. 2008, WHO 2009).

Five genera of the *Caliciviridae*

The members of the *Caliciviridae* family are distributed into five genera based primarily on genetic relatedness: *Vesivirus, Lagovirus, Sapovirus*, *Norovirus* and the recently accepted genus *Nebovirus* (ICTV, King et al. 2012).

The *Nebovirus* genus, named after the town Newbury, United Kingdom, is composed of one member – Newbury-1 virus. Newbury-1 virus (also called or Newbury agent 1 virus) was isolated from the feaces of a calf with acute enteritis in 1978 (Woode and Bridger 1978). Neboviruses are reported to cause enteric-related diseases such as diarrhoea, anorexia, severe small intestine lesions and malabsorption of some nutrients (Bridger, Hall et al. 1984).

The *Norovirus* genus contains memebrs that are related genetically and serologically to the Norwalk virus. Norwalk virus was first recovered in 1968 from an outbreak in Norwalk, United States of America, hence the name of the genus (Adler and Zickl 1969). Human norovirus are a major cause of gastroenteritis; they are commonly referred as the winter vomiting bug, leading to episodes of diarrhoea and vomiting (Patel, Hall et al. 2009). Other noroviruses have been described in other animals, including cows, pigs and dogs, causing enteric diseases (Wang, Han et al. 2005, Mattison, Shukla et al. 2007, Martella, Lorusso et al. 2008, Di Bartolo, Ponterio et al. 2011).

The *Sapovirus* genus is composed by members who are related to the Sapporo virus, which was first isolated in an outbreak in 1977, in a Japanese city called Sapporo (Chiba, Sakuma et al. 1979). Human sapovirus causes gastroenteritis in humans and generally infect children and the elderly (Pang, Lee et al. 2009). Sapoviruses can also infect pigs causing enteric diseases (L'Homme, Brassard et al. 2010).

The *Lagovirus* genus contains two viruses that affect lagomorphs, hence its name. The RHDV infects rabbits causing virulent disease and symptoms described as heamorrhagic, pneumotic and hepatic lesions with high mortality (Ohlinger, Haas et al. 1990). The other virus of the genus is the *European brown hare syndrome virus* (EBHSV).

This virus was first identified in Sweden and forms lesions in the liver and also has a high mortality rate (Wirblich, Meyers et al. 1994).

Lastly, in the *Vesivirus* genus two viruses are recognized: FCV and VESV. VESV it is known to infect pigs causing the formation of vesicles in the mouth, nose, trotters and ears as well as fever (Smith, Akers et al. 1973). SMSV is another vesivirus that induce similar symptoms in sea lions. Cross-species infection of SMSV in marine mammals and pigs has also been reported; these viruses are phylogenetically close and it is thought that they evolved in the same marine reservoir (Smith, Akers et al. 1973, Smith, Skilling et al. 1998).

The study of human caliciviruses has been hampered by the lack of an efficient propagation system in cell culture. However, some exceptions exist. FCV has been studied for several decades, since it can be propagated in Crandell-Reese feline kidney (CRFK) cells and feline embryonic fibroblasts (FEA) (O'Reilly 1969, Khan, Kociba et al. 1992). In 2004, Wobus and colleagues were able to propagate a member of the *Norovirus* genus – the murine norovirus (MNV) – in macrophage-like cells (Wobus, Karst et al. 2004). Since then, MNV has been used as a surrogate model to study human calicivirus biology and pathogenesis (Wobus, Thackray et al. 2006, Leung, Chan et al. 2010). In recent years, porcine enteric calicivirus (PEC) - a sapovirus – has been successfully propagated in cell culture. Considering it is an enteric calicivirus that causes a disease that resembles human calicivirus, PEC has also been proposed a surrogate model for human noroviruses and sapoviruses (Chang, Kim et al. 2002, Vashist, Bailey et al. 2009).

Within this dissertation, FCV and human sapovirus are investigated by electron microscopy to understand the structure of their capsids, how they interact with cellular receptors and the structural changes to the cell result from virus infection.

2. Feline calicivirus Infection

FCV is one of the most important and studied models for calicivirus infection. The infection is thought to be restricted to felids. In cats, FVC infection is a major cause of respiratory disease with high prevalence in catteries and shelters (Coyne, Dawson et al. 2006).

Pathology

Symptoms of FCV infection include pneumonia, acute conjunctivitis, rhinitis, and tracheitis, accompanied by the ulceration of the oral epithelium (stomatitis – mainly affecting the mouth and tongue). Infections with less virulent strains are symptomatically confined to lesions in the upper respiratory tract, eyes and oral cavity. Oral ulceration is the most common symptom of an FCV infection (Hoover and Kahn 1975, Radford, Coyne et al. 2007). Other common symptoms are fever, lethargy, and anorexia. Although FCV can quickly spread among a cat population, mortality is usually low (Radford, Coyne et al. 2007). Virulent strains of feline calicivirus (VS-FCV), however, have higher mortality rates ranging from 33 to 60% (Pedersen, Elliott et al. 2000, Hurley, Pesavento et al. 2004). VS-FCV usually causes severe pneumonia, subcutaneous edema, alopecia, and prominent ulceration of the paws, nose and ears. Vesicles in the tongue, gingiva, palate and nasal cavity develop quickly into ulcers with a healing time of 2-3 weeks. Other symptoms have been found in experimentally infected cats, such as pulmonary edema and parenchymal necrosis in the liver, spleen and pancreas (Schorr-Evans, Poland et al. 2003, Pesavento, MacLachlan et al. 2004, Reynolds, Poulet et al. 2009).´

FCV antigens has been identified by immunohistochemistry in skin, nasal, and oral lesions, and necrotic epithelial areas of both lungs and pancreas (Radford, Coyne et al. 2007). VS-FCV antigens have also been associated to endothelial cells, which explains the vascular injury caused by VS-FCV infection (Pesavento, MacLachlan et al. 2004). In cell culture, FCV cytopathic effect has been extensively characterized as cell rounding, membrane fragmentation and the formation of membrane-bound vesicles in the cytoplasm, this latter phenomenon being characteristic of infections caused by positive-sense RNA viruses (Love and Sabine 1975, Studdert and O'Shea 1975). Recently, Abente and colleagues identified the leader of the capsid (LC) protein of FCV as the protein that induces this characteristic cytopathic effect (Abente, Sosnovtsev et al. 2013). Inhibition of

cellular protein synthesis also occurs, and in FCV-infected cells the mitochondrial apoptosis pathway is activated which leads to cellular apoptosis (Willcocks, Carter et al. 2004, Natoni, Kass et al. 2006). Interestingly, FCV replication and *de novo* synthesis of virus proteins are essential for induction of apoptosis (Sosnovtsev, Prikhod'ko et al. 2003).

Epidemiology

Infection by FCV is widespread in the cat population (Harbour, Howard et al. 1991, Porter, Radford et al. 2008). Prevalence values range between 15 to 20%, for cats visiting veterinary facilities, and 70 to 90% in shelters (Bannasch and Foley 2005, Coyne, Dawson et al. 2006). Studies found a proportional relationship between population density and prevalence within the population (Radford, Coyne et al. 2007). Evolution of the virus within cats and subsequent re-infection of convalescent cats combined with long-term shedders can contribute to the high prevalence values described in denser cat populations (Hurley, Pesavento et al. 2004, Coyne, Gaskell et al. 2007, Pesavento, Chang et al. 2008). FCV recombination within a colony has also been reported, which supports the hypothesis of re-infection (Coyne, Reed et al. 2006). FCV may also survive in fomites for several days at room temperature, or longer if kept in colder and wetter conditions (Doultree, Druce et al. 1999, Clay, Maherchandani et al. 2006). These data suggest that indirect transmission can also occur, and it was reported to be critical in VS-FCV outbreaks (Reynolds, Poulet et al. 2009).

There are no recognized reservoirs or alternative hosts for FCV (Radford, Coyne et al. 2007). It has been suggested, however, that canines may be an important source of FCV: it has been reported that FCV-like viruses were present in dogs with mild enteritis (Hashimoto, Roerink et al. 1999, Martella, Pratelli et al. 2002, Di Martino, Di Rocco et al. 2009). In another study, canine calicivirus isolated from faecal samples of dogs was shown to differ genetically and antigenically from FCV (Mochizuki, Kawanishi et al. 1993). There have however been studies showing that FCV is indeed widespread in dog populations and that contact with dogs is a risk factor for FCV infection (Binns, Dawson et al. 2000, Di Martino, Di Rocco et al. 2009). Considering that SMSV can infect several marine mammals and pigs (Berry, Skilling et al. 1990), inter-species transmission of FCV is considered likely although further investigation on the matter is required.

Transmission and Tropism

FCV is shed by cats through oropharyngeal secretions and nasal aerosols; however, contact with fomites or human handlers may also infect susceptible cats (Radford, Coyne et al. 2007). Carriers are defined as those cats that shed beyond 30 days. In some cases, individual cats can shed for life, although most infected cats cease shedding 75 days after inoculation (Coyne, Dawson et al. 2006). The majority of long-term shedders are cats that are re-infected with either different variants of the same strain or different strains of FCV; while some other cats that are re-infected with the same lineage of virus can act like a reservoir for the household population (Coyne, Dawson et al. 2006).

Other methods of propagation have also been suggested. In 2009, Mencke *et al.* observed that cat fleas (*Ctenocephalides felis*) were able to spread infectious virus through their faeces or by bite (Mencke, Vobis et al. 2009).

FCV is known to infect the epithelial cells of the nose, lung, pharynx, trachea and eye (Hoover and Kahn 1975). Although FCV has been described to bind poorly to other cells beside feline cells, studies showed that transfection of viral RNA leads to FCV replication (Kreutz, Seal et al. 1994, Sosnovtsev and Green 1995, Pesavento, Chang et al. 2008). Such findings suggest that host range restriction is determined early in the infectious cycle, before delivery of the viral genome. Two molecules have been identified as FCV receptors: the feline junction adhesion molecule A (fJAM-A) and the α-2,6 sialic acid (Makino, Shimojima et al. 2006, Stuart and Brown 2007). fJAM belongs to the family of immunoglobulin-like molecules and plays an important role in the assembly and maintenance of tight junctions and the establishment of epithelial cell polarity (Martin-Padura, Lostaglio et al. 1998). Recently, Pesavento *et al.* have shown that fJAM-A has an extensive distribution in feline tissues, localized in epithelial and endothelial cell-cell junctions, and feline platelets (Pesavento, Stokol et al. 2011). Unlike fJAM-A, the presence of α-2,6 sialic acid on cell surfaces is insufficient to mediate infectious entry (Stuart and Brown 2007).

Genomic and Antigenic Diversity

As commonly reported for positive sense RNA viruses, FCV has a high mutation rate which results in significant variability at the genomic and antigenic levels. Several studies stated that a cat colony can develop their own strains of FCV with variation rates of 15 to 20% in predominant antigenic sites (Radford, Dawson et al. 2003, Coyne, Christley et al. 2012).

Strains of FCV belong to only one genogroup. Diversity of the FCV genome has been observed within the group, however subspecies clustering is not believed to occur. Along with the genetic diversity of FCV, antigenic diversity is also considerable. Some studies, though, state that the observed cross-reactivity of all isolates is sufficient to classify them as a single serotype (Povey and Ingersoll 1975, Coyne, Christley et al. 2012).

Several studies on the evolution of FCV in individual infected cats showed that substantial changes in virus neutralization profile can arise from a single parental strain of FCV. Successive passages in virus culture did not present this kind of profile, suggesting that positive selection mediated by the immune system contributes to FCV antigenic change (Kreutz, Johnson et al. 1998, Radford, Turner et al. 1998). Interestingly, it has been suggested that selection carried out by the immune system can lead to the establishment of a persistent infection.

Coyne *et al.* estimated the evolutionary rates of the variable regions of the capsid protein to be 1.3 to 2.6 $\times 10^{-2}$substitutions per nucleotide per year – considered one of the highest evolutionary rates ever reported for a virus (Coyne, Gaskell et al. 2007). The same laboratory described, in 2012, the first phylodynamics study of a calicivirus at national scale, suggesting that FCV evolution is not associated with selective competition among strains, but its genetic and antigenic profile is confined to a geographical location (<100km) and is composed of several strains that co-circulate (Coyne, Christley et al. 2012).

Diagnosis, Treatment and Prevention

Diagnosis is generally accomplished through the combined findings of three approaches: (1) clinical presentation, (2) virus isolation in cell culture or Reverse-Transcriptase-PCR (RT-PCR) assay and (3) serological assays (Pesavento, Chang et al. 2008). Other diseases, such as feline rhinotracheitis, can be confused with milder forms of FCV infection. Due to the low correlation between the presence of virus and the manifestation of clinical signs in FCV infected cats (*e.g.*, the asymptomatic carrier phase), and the propensity of cats to shed following vaccination, caution should be taken in diagnosis (Sykes, Studdert et al. 1998, Ruch-Gallie, Veir et al. 2011). Thus, combining the clinical presentation with virus identification is essential to obtain a correct diagnosis. RT-PCR assays are used to detect viral RNA in blood samples, oral swabs or lung tissue. Although this test is sensitive (depending on the set of primers used), RT-PCR can fail to detect FCV due to the high variability of its genome. Still, this test is the most effective for detection of variant strains of FCV (Radford, Addie et al. 2009). On the other hand, virus isolation in cell culture can be advantageous since this method is less sensitive to FCV variability, when compared to RT-PCR. This method depends on the ability of FCV to infect certain cell lines in culture. Virus is isolated from oral, conjunctival or nasal swabs. A major drawback of this method is that the number of viable virus particles found in a swab may sufficient to induce cytopathic effect *in vitro*. This may be because of poor sample preservation or or the presence of neutralizing antibodies that can prevent FCV replication in tissue culture (Marsilio, Di Martino et al. 2005, Radford, Addie et al. 2009). Finally, FCV presence can be detected through serological studies, in which virus antibodies are identified using enzyme-linked immunosorbent assay (ELISA) or virus neutralization. However, in vaccinated or pre-infected cats levels of FCV antibodies are generally high, which can lead to misdiagnosis (Gore, Lakshmanan et al. 2006).

As previously described, FCV infection presents a wide range of symptoms, so treatment should be specific for the symptoms and strains involved in the infection. Acute upper respiratory tract disease is common to all FCV infections; in its treatment, electrolyte replenishment and rehydration are essential, as well as the use of anti-inflammatory drugs to reduce fever and pain. Antibiotics directed to the respiratory tract and oral cavity are commonly used, to prevent secondary infection (Radford, Addie et al. 2009). Antivirals for FCV infection have not been identified yet. Studies showed that certain compounds can inhibit FCV replication *in vitro*: ribavirin – which is toxic for cats and is no longer used (Povey 1978) - and feline interferon-ω – are shown to be effective only against certain

strains (Taira, Suzuki et al. 2005, Ohe, Takahashi et al. 2008). In the treatment of stomatitis, corticosteroids, immunosuppressants or immunomodulatory drugs – such as clorambucil, thalidomide and cyclosporine - can be used (White, Rosychuk et al. 1992, Addie, Radford et al. 2003). Treatment for VS-FCV infection is not available. Some reports have noted that intensive care with steroids and interferon treatment may lead to clinical improvement (Hurley 2006 adapted from Radford, Addie et al. 2009).

The control of FCV infection is highly dependent on vaccination. Different vaccines are commercially available; most are live-attenuated or inactivated adjuvanted and are administered intramuscularly or intranasally (Radford, Dawson et al. 2006). Considering strain variability and the adaptability of FCV, producing an efficient multi-strain vaccine has been challenging. Conventionally, the vaccines in use are developed from a single strain – most commonly strains FCV-F9 or FCV-255 (Bittle and Rubic 1976, Povey, Koonse et al. 1980). Recently developed vaccines are based upon two (Poulet, Brunet et al. 2005) or three strains (Masubuchi, Wakatsuki et al. 2010). It is believed that a vaccine based upon a greater number of strains can grant a better protection against circulating wild-type FCV (Addie, Poulet et al. 2008, Huang, Hess et al. 2010). Other vaccines, such as Leucofeligen, are tetravalent vaccines against several different viruses – FCV, *Feline herpersvirus*, *Feline panleukopenia virus*, and *Feline leukaemia virus* – and have been shown to provide vaccinated kittens with increased protection against virulent strains of FCV (Lesbros, Martin et al. 2013).

Despite vaccination, infection levels have not been reduced (Gaskell, Gaskell et al. 1982, Coyne, Christley et al. 2012) –these vaccines are, however, considered effective at reducing the clinical signs of oral and respiratory disease (Radford, Dawson et al. 2006).

3. Feline calicivirus Genome Organization and Viral Proteins

Genome

FCV has a positive-sense RNA genome. RNA viruses have higher mutation rates – when compared to DNA viruses – granting them the ability to evolve more quickly, enhancing their chances of survival in the face of host defences (Domingo, Menendez-Arias et al. 1997, Moya, Holmes et al. 2004). This high mutation rate has been attributed to the fact that the polymerase assembles the nascent RNA molecule without any proofreading activity (Steinhauer, Domingo et al. 1992, Elena and Sanjuan 2005). Studies demonstrated that RNA viruses have an average mutation rate of 1 mutation per genome per replication (Drake 1993). As previously stated, calicivirus mutation rates are among the highest amongst RNA viruses (Nilsson, Hedlund et al. 2003, Coyne, Gaskell et al. 2007, Victoria, Miagostovich et al. 2009), contributing to the plasticity of its genome and wide variation of genotypes.

The FCV genome is a linear, polyadenylated single-stranded positive sense RNA molecule that is approximately 7.7 kilo base pairs (kbp) in length (Carter, Milton et al. 1992). It comprises three open reading frames (ORFs): ORF1 (nucleotides 20 to 5308), ORF2 (5314 to 7317) and ORF3 (7317 to 7634) (**Fig1.1**) (Sosnovtsev, Garfield et al. 2002). Infected cells generally present two types of viral RNA: the genome and a subgenomic molecule of 2.4kbp. This subgenomic RNA corresponds to ORFs 2 and 3 (Neill and Mengeling 1988, Neill, Reardon et al. 1991).

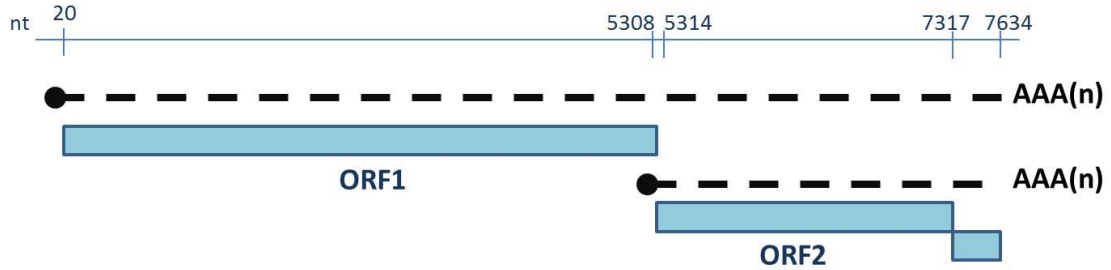

Figure 1.1 – Schematic representation of the FCV genome and ORFs. The dashed lines indicate the genome and subgenomic RNAs. VPg is depicted as a filled circle at the end of dashed lines. The three ORFs are represented as blue rectangles in association to their position in the genome. The numbers above indicate the nucleotide where each ORF begins and ends.

Another feature of caliciviruses is that the capsid and non-structural proteins are encoded in distinti and seperate ORFs (Clarke and Lambden 1997). ORF1 encodes a polyprotein that is later cleaved into six proteins (Sosnovtsev, Garfield et al. 2002). Most of these proteins are non-structural proteins, which mean that they are not found in mature assembled virus particles. The only exception is a viral protein that is found linked to the genome (VPg). ORF1 also encodes a nucleotide triphosphatase (NTPase) and a proteinase polymerase (Pro-Pol) (Herbert, Brierley et al. 1997, Wei, Huhn et al. 2001, Sosnovtsev, Garfield et al. 2002). Three further proteins are synthesized – designated p5.6, p30, and p32 – their function, however, is still unknown. Structural proteins are encoded by ORF2 and 3. ORF2 encodes the precursor for the major viral capsid protein (VP1) with a leader capsid (LC) sequence (Carter 1989). ORF3 encodes a minor capsid protein (VP2), which is found in low quantity in mature virus particles (1 or 2 copies per virion) (Carter 1989). Gene overlapping occurs only at the ORF2/ORF3 interface, in which the termination codon of ORF2 overlaps the start codon of ORF3 by four nucleotides (Clarke and Lambden 1997).

Nonstructural Proteins

The FCV genome encodes both structural and non-structural proteins. Non-structural proteins mediate virus replication in the host and are encoded in ORF1. Pro-pol is a precursor protein which, after cleavage, becomes the mature proteinase and the RNA-dependent RNA polymerase (RdRp). RdRps play a critical role in virus replication and are found in all positive sense RNA viruses (O'Reilly and Kao 1998). The main function attributed to the viral proteinase is the cleavage of the polyprotein translated by the ORF1 and the cleavage of the precursor capsid protein (Sosnovtsev, Sosnovtseva et al. 1998, Sosnovtseva, Sosnovtsev et al. 1999). Kaiser *et al.* observed that the immature form of the pro-pol protein can form homo-oligomers and it interacts with VPg and the ORF2 (Kaiser, Chaudhry et al. 2006). A similar activity has been described for RHDV, which suggests that this phenomenon may play an important role in the replication of caliciviruses (Ng, Cherney et al. 2002).

VPg is a ~14kDa protein which is covalently linked to the 5' terminus of the FCV genome or subgenome (Burroughs and Brown 1978, Schaffer, Ehresmann et al. 1980). VPg was found to be required for translation initiation, acting as a cap for ribosomal recruitment (Sosnovtsev and Green 1995, Herbert, Brierley et al. 1997). More recent studies demonstrated that VPg interacts with the cap-binding protein eukaryotic initiation factor 4E (eIF4E). This protein is involved in the first step of translation binding to 5'capped mRNAs (Gingras, Raught et al. 1999). Its interaction with VPg suggests that caliciviruses use translation initiation factors to recruit the ribosome (Goodfellow, Chaudhry et al. 2005, Chaudhry, Nayak et al. 2006). Furthermore, VPg can be nucleotidylated by the viral pro-pol, generating a template that may be involved in genome replication (Rohayem, Robel et al. 2006, Belliot, Sosnovtsev et al. 2008). This interaction though appears to be different among genera (Leen, Kwok et al. 2013). A study published by Kaiser *et al*. showed that VPg also interacts with VP1, suggesting a putative role in viral RNA packaging during virus particles assembly (Kaiser, Chaudhry et al. 2006).

Three further non-structural proteins are encoded by ORF1: p5.6, p30, and p32 – designated according to their molecular weight, 5.6kDa, 30kDa, and 32kDa, respectively. The function of these three proteins is unknown; however some studies indicate that p30 and p32 may play a role in the formation/activity of FCV replication complexes. Green *et al.* in 2002, identified both p30 and p32 in enzymatically active replication complexes isolated from FCV-infected cells (Green, Mory et al. 2002). In this study, p30 and its precursor form (p30-VPg) are shown to accumulate in replication complexes over time.

Additionally, owing to the similarity between polioviruses and caliciviruses, a parallel is established between p30 and its homologue in poliovirus (3A protein), which has been proposed to be anchored in membranes so that VPg is appropriately positioned for RNA replication (Datta and Dasgupta 1994, Lama, Paul et al. 1994, Towner, Ho et al. 1996). In 2010, Bailey *et al.* demonstrated that p30, p32 and NTPase proteins locate to the endoplasmic reticulum (ER), leading to ER membrane reorganization similar to the patterns observed in FCV-infected cells (Bailey, Kaiser et al. 2010). Collectively, these data suggest that p30 and p32 play a role in FCV RNA replication.

Structural Proteins

Structural proteins are those that are found in mature virions. In the case of FCV, there are only two desingated structural proteins: VP1, which is encoded by ORF2, and VP2, encoded by ORF3. ORF2 encodes a precursor capsid protein that is post-translationally cleaved to release two products: VP1 and the 'leader of the capsid' (LC) protein. The expression of VP1 from a precursor protein is a unique feature of the *Vesivirus* genus (Fretz and Schaffer 1978, Carter 1989). Infectious virus particles can not be recovered when this cleavage is inhibited, suggesting that VP1 is only functional following removal of the LC (Sosnovtsev, Sosnovtseva et al. 1998). LC is a protein of 124 amino acids of which the function is unknown. A recent study demonstrated that cells transiently expressing wild-type LC protein, showed a cell-rounding phenotype typical of *in vitro* FCV infected cells (Abente, Sosnovtsev et al. 2013). The same study also found that LC binds to the host cellular protein annexin A2 – a protein associated with the cytoskeleton and cell motility (Gerke and Moss 2002) – suggesting that the LC-annexin A2 interaction may change the structure of the cell, to favour virus replication. Interestingly, LC was shown to promote the replication of Norwalk virus in cell culture, supporting the idea that LC is required for efficient replication of feline calicivirus (Chang, George et al. 2008).

ORF2 is divided into six regions with respect to its degree of conservation among species (Neill 1992, Radford, Willoughby et al. 1999). These regions are designated from A to F: region A is the LC that has been described above, which shows a moderate degree of variability between species except for the cleavage site which is highly conserved (Glenn, Radford et al. 1999). Regions B, D and F have been reported to be the most conserved parts of VP1, suggesting that they are functionally important (Neill 1992). In particular, region B has an ATP/GTP binding motif with homology to picornavirus VP3 protein, which has been shown to be essential for virus survival (Tohya, Taniguchi et al. 1991, Seal, Ridpath et al. 1993, Seal 1994). VP1 has a molecular mass of 60kDa and is divided into three domains: an N-terminal arm (NTA), the shell (S) domain and the protruding (P) domain (**Fig1.2A**). The NTA faces the interior of the capsid; the S domain forms the capsid surface; and the P domain is projected outwards from the capsid floor. Additionally, the P domain is divided into two subdomains, designated P1 and P2. P1 is proximal to the S domain; while the P2 domain is distal to the capsid shell and on the outermost surface of the viral particle (Prasad, Matson et al. 1994, Prasad, Hardy et al. 1999, Chen, Neill et al. 2006). The P2 domain is therefore the region where most of the

neutralizing epitopes are located (Matsuura, Tohya et al. 2001, Geissler, Schneider et al. 2002).

The second protein found in FCV virions is VP2 which is encoded by ORF3. VP2 is a 12kDa protein and its function is unknown. Sosnovtsev and colleagues showed that ORF3 deletion is lethal to FCV. Furthermore several mutations were made in this region, that abolished virus replication (Sosnovtsev, Belliot et al. 2005). It has also been demonstrated that co-expressing VP1 and VP2 generates FCV VLPs that more closely resemble wild-type virions compared to the single expression of VP1, suggesting a role for VP2 in the correct assembly of FCV particles (Di Martino, Marsilio et al. 2007, Di Martino and Marsilio 2010).

The calicivirus capsid consists of 180 copies of VP1, organized into 90 arch-like dimers which give caliciviruses their characteristic morphology (Prasad, Matson et al. 1994) (**Fig1.2B**). VP1 dimers are arranged according to a T=3 icosahedral symmetry, originating from three quasi-equivalent environments Consequently VP1 monomers fall into three distinctive equivalent conformations – designated A, B and C. VP1 dimers are distributed in two classes: AB dimers, arranged around the 5-fold axes, and CC dimers, located at the 2-fold axes (Prasad, Hardy et al. 1999).

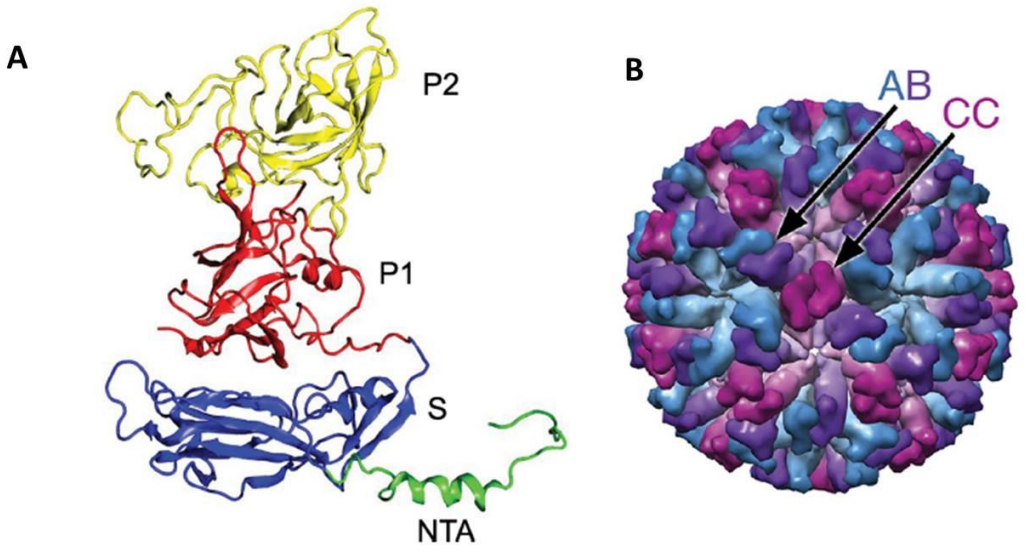

Figure 1.2 - VP1 monomer and capsid assembly. (A) X-ray structure of VP1 of FCV-5, ribbon representation. The N-Terminal Arm (green), Shell domain (blue), and P1 (red) and P2 (yellow) subdomains are indicated (Ossiboff *et al.* 2010). (B) T=3 icosahedral capsid formed from VP1 assembly, represented in three quasi-equivalent environments: A (blue), B (purple) and C (magenta). VP1 dimers: AB and CC. (Bhella *et al.* 2008)

The viral capsid has a variety of functions and is fundamental for the life cycle of the virus. It is responsible for attachment and entry: delivering the viral genome across the host cell plasma membrane into the cytoplasm. The capsid must also specifically package progeny viral genomes to form new virions. The viral capsid must also prevent genome damage, protecting it from the harsh extracellular environment during transmission from host to host. Studies have shown that the FCV capsid is moderately stable, maintaining infectivity following exposure to harsh environmental conditions: in a pH range of 4 to 8.5 (Pesavento, Chang et al. 2008) and temperature range (Topping, Schnerr et al. 2009); additionally, as previously mentioned, FCV can survive in fomites for several days or weeks. Thus the viral capsid protein must be capable of forming a robust shell that is nonetheless sufficiently dynamic to package the viral genome and then uncoat upon arrival in specific compartments of the new host cell.

4. FCV life cycle

Host Cell Recognition and Cell Entry

Host cell recognition and cell entry are two critical steps in a virus's life cycle. In the case of FCV infection, susceptibility has been demonstrated to be conferred on non-permissive cells by exogenous receptor expression. Understanding the early stages of infection is therefore of fundamental importance a target for potential antiviral intervention.

Two molecules have been described as receptors for FCV: fJAM-A and α-2,6 sialic acid. Despite α-2,6 sialic acid having the ability to enhance FCV binding at the cell surface, it can not mediate virus entry by itself; on the other hand, fJAM-A expression on nonpermissive cells renders them susceptible to infection (Makino, Shimojima et al. 2006, Stuart and Brown 2007). fJAM belongs to the family of immunoglobulin-like molecules and is important in the assembly and maintenance of tight junctions and the establishment of epithelial cell polarity (Martin-Padura, Lostaglio et al. 1998). Pesavento *et al.* have shown that fJAM-A has an extensive distribution in feline tissues, localized in epithelial and endothelial cell-cell junctions, and feline platelets (Pesavento, Stokol et al. 2011). During FCV infection, fJAM relocates to the cytosol, as a result of FCV binding and tight junction disruption; furthermore, this disruption induced by FCV is thought to promote the cell rounding phenotype in FCV infection. fJAM-A is a transmembrane protein composed of five domains: the N-terminal signal peptide; two immunoglubin-like domains designated D1 - positioned farthest from the membrane – and D2 – closer to the membrane; the C-terminal transmembrane domain; and the cytoplasmic domain (Kostrewa, Brockhaus et al. 2001). Ossiboff and colleagues identified D1 as the main domain for FCV interaction; the same study identifies several critical amino acids for FCV infection (Ossiboff and Parker 2007). Bhella *et al.* showed that the D1 domain of fJAM-A interacts with the P2 domain of VP1 of FCV, and the region involved in this interaction possesses several neutralizing epitopes (Bhella, Gatherer et al. 2008). The same laboratory showed later that interactions with FCV and fJAM-A lead to a group of conformational changes in the virus capsid that might represent the initial steps of virus uncoating (Bhella and Goodfellow 2011). In particular, this study showed that binding of the P domain of VP1 to fJAM-A leads to a loss of the icosahedral symmetry in the capsid. They observed two distinctive

conformation changes: (1) the P domain of the CC dimers tilts away from the 2-fold axis while (2) in AB dimers, the P domain rotates from its unbound position by 15°.

Intracellular Pathway

The way small nonenveloped positive-sense RNA viruses penetrate cells and release the genome is poorly understood (Tsai 2007). However, two studies have explored the entry pathway of FCV. In 1995, Kreutz and Seal demonstrated that FCV infection is dependent on the low-pH environment of endosomes (Kreutz and Seal 1995). Endosomal pH normally ranges from 5.2 to 6.7 depending on the cell line in use (Rybak and Murphy 1998, Gagescu, Demaurex et al. 2000). Additionally, Stuart and Brown showed, using drugs that inhibit different endocytic pathways, that FCV uptake occurs by the clathrin-mediated pathway (Stuart and Brown 2006). This pathway is critical for receptor-mediated endocytosis, and involves the formation of complex structures – coated pits – at specific sites of the cell membrane (Mousavi, Malerod et al. 2004). The formation of coated pits involves the interaction of several proteins, most importantly clathrin and an adaptor protein called AP-2. Clathrin assembly units are called triskelion because its structure resembles the three interlocked spirals found, for example, in the Isle of Man flag (Liu, Wong et al. 1995). AP-2 is composed of four subunits and its function is to coordinate the coated pit formation, binding to cargo proteins, the vesicle lipid bilayer and clathrin (Pearse, Smith et al. 2000). After the clathrin lattice is formed, the vesicle buds out from the cell membrane (Mousavi, Malerod et al. 2004). Clathrin-coated vesicles lose their clathrin coat after separation from the cell membrane and bind to microtubules to be transported to early endosomes (Sorkin 2000). As mentioned above studies demonstrated pH dependency of FCV uncoating. Virions must escape the endosome before it fuses to lysosomes initiating protein degradation. Tsai divides this process in four steps: (1) virus must be located to the membrane penetration site, (2) where cellular components and certain environmental conditions, such as low pH, receptors, proteases, chaperones, etc.) may impart new characteristics that (3) enable it to disrupt the endosome membrane and (4) to transport itself or only its genome into the cytosol (Tsai 2007). These new characteristics may include conformational changes that grant the virus a greater hydrophobicity or trigger the release of a viral fusion peptide that may disrupt the membrane. Such mechanisms are described for other nonenveloped virus: in poliovirus, after receptor binding, the N-terminal parts of two capsid proteins become exposed to the surface – the myristolated glycine of VP4 and the amphipathic helix of VP1 – and insert

into the membrane, leading to the release of the viral RNA genome into the cytoplasm (Paul, Schultz et al. 1987, Fricks and Hogle 1990, Danthi, Tosteson et al. 2003, Bostina, Levy et al. 2011); in reovirus infection, the attachment protein σ1 binds to its physiological receptor, JAM-A, inducing its homodimerization. Virus is internalized in the endocytic compartment, where host proteases cleave another capsid protein, σ3, exposing the viral membrane-penetration protein μ1. Finally, this protein is cleaved and locates to the endosomal membrane, inducing its disruption and causing the virions to be released into the cytosol (Danthi, Guglielmi et al. 2010). The mechanism of membrane penetration for FCV has not been described yet. However, a study on FCV-fJAM-A binding showed that upon co-incubation with the soluble form of fJAM-A FCV increases in hydrophobicity (Ossiboff, Zhou et al. 2010), suggesting that conformational changes in the FCV capsid may be important for membrane penetration and genome delivery. In this dissertation, the role of low-pH in inducing conformational changes in the FCV capsid is explored.

Translation and Replication Strategy

FCV protein synthesis is thought to occur via a unique mechanism different from that of any other animal RNA virus. FCV translation occurs through the recruitment of ribosomes by VPg. As set out above, VPg is covalently linked to the FCV genome (at the 5' end) and it has been demonstrated that VPg recruits eIF4E and eukaryotic translation ignition factor 3 (eIF3) (Goodfellow, Chaudhry et al. 2005).

Both 5' and 3' ends of the viral genome have been implicated in regulation of viral translation and replication (Ahlquist, Noueiry et al. 2003). Karakasiliotis and colleagues showed in 2006 that a polypyrimidine tract binding (PTB) protein binds to the 5' end of FCV genome, and is required for FCV life cycle in a temperature-dependent manner (Karakasiliotis, Chaudhry et al. 2006). The PTB protein contains four RNA recognition motifs with affinity for RNA sequences rich in pyrimidines (Auweter, Oberstrass et al. 2007). It is classified as an RNA chaperone and its interaction with target RNA may help to fold the viral RNA into functional structures (Mitchell, Spriggs et al. 2003). The same laboratory showed recently that host PTB protein relocates from the nucleus to the cytoplasm during FCV infection and functions as negative regulator of FCV translation (Karakasiliotis, Vashist et al. 2010). Furthermore, it is proposed that PTB may work as a switch mechanism from translation to replication during FCV infection. Another recent study showed that nucleolin interacts with the 3' untranslated region of FCV and with the pro-pol protein, and relocates from the nucleoli to the nucleoplasm and the perinuclear space (Cancio-Lonches, Yocupicio-Monroy et al. 2011). Furthermore, the same study has demonstrated that nucleolin knockdown by small interfering RNA was deleterious to FCV replication.

For many positive-stranded RNA viruses, it has been shown that infection leads to the formation of membraneous vesicles in the cytoplasm and that these vesicles are sites of viral RNA synthesis (den Boon and Ahlquist 2010). These membraneous structures are also referred to as replication complexes therefore. Poliovirus was shown to reorganize the membranes of the Golgi, endoplasmic reticulum, and lysosomes into clusters of vesicles (Bienz, Egger et al. 1990, Egger, Teterina et al. 2000) and RNA replication was found to occur in ER-derived membranes or in membranes resultant from the autophagy process (Rust, Landmann et al. 2001, Jackson, Giddings et al. 2005). In 1975, two studies first described membrane-bound vesicles in feline kidney cells infected with FCV. (Love and Sabine 1975, Studdert and O'Shea 1975) Studdert and O'Shea reported that these

vesicles were frequently found in the centre of the infected cell, normally in large amounts and with a dark-staining core. Love and Sabine observed that these vesicles could be single or double membraned, with variable size and granularity. Although these structures found in FCV infected cells resemble the replication complexes of other RNA viruses, their composition, function and formation are poorly understood (Bailey, Kaiser et al. 2010). Nonetheless, it has been shown that all of the machinery necessary for viral RNA replication is associated with these membranes, in particular the non-structural proteins synthesized and processed from ORF1, p30, p32 and the NTPase (Green, Mory et al. 2002). Exogenous expression of these proteins, which are predicted to be transmembrane in nature, led to their accumulation in the ER resulting in ER deformation and the formation of similar membranous structures to those found in FCV infected cells (Bailey, Kaiser et al. 2010). In this dissertation we have used 3D electron microscopy to investigate the structures and origins of these compartments.

5. Cryo-Electron Microscopy and Icosahedral Reconstruction

Electron microscopy (EM) has been a fundamental tool in biological sciences. A transmission electron microscope (TEM) is a microscope that uses a beam of electrons to observed specimens in great detail. In 1931 Ernst Ruska built the first TEM, which was used in 1939 to observe the first virus under TEM, the tobacco mosaic virus (Kausche, Pfankuch et al. 1939).

Interaction between biological material and electrons

The fact that electrons have a short wavelength is determinant to the visualization of high-resolution molecular features. Still, the interaction between electrons and samples may not be suitable to observe structural details, due to loss of the stability of the sample. Biological specimens must be kept in high vacuum once inside microscope and may lose their natural conformation (Jensen 2010, Grishaev 2012). This problem can be solved by cryo-EM. In this procedure, samples are maintained stable and in the hydrated state. In this type of microscopy specimens in aqueous solution are frozen into liquid ethane, which liquefies under -182°C and is usually kept in the liquid state by liquid nitrogen (-196°C). This enables the specimen to be kept in its natural state and grants some protection to radiation damage of the sample (Dobro, Melanson et al. 2010).

Biological material is usually bound to carbon support films. However, carbon films are not translucent to the electron beam, adding background scattering to the image, reducing its contrast. To overcome this situation, perforated carbon support films are commonly used – samples located in the “hole” regions are suspended in ice, where they can be imaged with less interference. With this technique, the ice film needs to have the correct size: a very thin layer of ice would make the sample collapse, whereas thick films of ice would decrease the contrast of the image (Orlova and Saibil 2011).

Three possible scenarios are known for the interactions of electrons with the sample: (1) electrons can pass directly through the sample suffering no deflection, (2) they may be deflected due to the electrostatic field of the nucleus (of the atoms) in the specimen; or (3) electrons can directly collide, hence suffering great deflection in their path. When an electron interacts with the samples, it can either lose or maintain energy; such a phenomenon is designated inelastic and elastic scattering, respectively. In these interactions, electrons can alter the nature of the sample – ionizing atoms, inducing chemical bond rearrangements, free radical formation – in a process called radiation

damage. This is a major drawback for high-resolution imaging. Still, most damage occurs at higher exposures - normally a range from 1 to 20 electrons/$Å^2$ is used in biological specimens (Orlova and Saibil 2011).

Functional parts of a Transmission Electron Microscope

A microscope can essentially be divided into three different functional parts: an electron source, a lens scheme and a system for image detection. The most common electron source is a tungsten filament that is heated between 2000 to 3000°C; in this state, the energy of the electrons at the surface of the filament is greater than the work-function of tungsten – *i.e.* the thermodynamic work required to remove an electron from tungsten. After this step, electrons are accelerated by an electric field (Chen, Liang et al. 2012). Subsequently, diverging electrons pass through a system of lenses whose major function is to condense the beam using an electro-magnetic field into a parallel beam. The lens system is very sensitive and can have several defects (*e.g.* chromatic, spherical, and astigmatism aberrations) that are also common in optical phenomena (Orlova and Saibil 2011). The beam finally passes through the specimen, where deflected and non-deflected electrons are detected by an image detection system. Electron detectors can be found in two types: analogic and digital detectors. Photographic film is one example of an analogic electron detector and it was used mainly in the beginning of EM microscopy. As in photography, microscopy photographic films contain silver halide crystals that absorb radiation and change to a metastable state, conserving the image that is later observed when the crystals precipitate during photographic development. Digital detectors, however, allow the systematic acquisition of data and are the most common electron detectors found in modern microscopy. Most digital detectors are based on a transducer system designated charge-coupled device (CCD); this system exploits photo sensors which transform light into an electrical charge. Moreover, since the high intensity electron beams can damage the photo sensors, scintillators are usually coupled to the CCD, in such a way that the scintillator absorbs the energy of the electron beam, and reemits the energy in the form of light which is subsequently received by the photo sensor. Still, the use of scintillators adds noise to the final image (Orlova and Saibil 2011, Wu, Zheng et al. 2012).

Compensation mechanisms for low contrast images

The resultant image is a representation of the detected electrons. However, as biological material contains mainly light elements (Hydrogen, Carbon, Oxygen and Nitrogen), electrons are only slightly deflected, and the number of electrons before and after the specimen is the same – generating low contrast images. To bypass this situation, microscopy takes advantage of the properties of the deflected electrons: as these have different path lengths after interaction with the specimen they exhibit different phase from those that did not interact with the sample. This phase shift is made visible by converting phase variation into amplitude variations. Still, phase shifts induced by biological samples generate very low contrast images. So, phase plates can be used to shift the phase of scattered light even more and induce an interference image (Glaeser 2008, Henderson and McMullan 2013).

Another consequence of inelastic scattering is that deflected electrons have lower energy, which means that these electrons have a longer wavelength. This wavelength gap between inelastic and elastic scattered electrons causes a chromatic aberration, corrupting the imaged with additional background and making it blurry. To correct this, energy filters are applied to the path of light after the specimen, deflecting electrons with different wavelength (Orlova and Saibil 2011). The usage of such filters substantially improves the contrast of the final image.

One simple method for increasing contrast is the manipulation of defects of lenses, in particular spherical aberrations, and the level of focus. Spherical aberration is an optical and electromagnetic effect characterized by the increased refraction of the beam, where refracted rays do not meet in one focal point. When the effect of spherical aberration and image defocus is combined, image contrast can be enhanced, since this combination leads to a phase shift between scattered and unscattered electrons (Henderson and McMullan 2013).

Tomography

Tomography is a variation of microscopy distinguished by a series of images of the same region over a range of tilt angles. Such procedure retrieves the information of several focus planes within an object that can be recovered to generate a three-dimensional reconstruction. One limitation of this technique is that tomograms (the result of a tilt series in tomography) will lack the information from a region in space: a wedge of ~50°, due to the extended path length of the beam through the samples. This effect is known as the missing wedge effect (Bartesaghi, Sprechmann et al. 2008). Moreover, during high tilt, inelastic scattering is increased, leading to a less coherent image. However, energy filters can be used to overcome this problem.

Processing

A drawback of improving contrast with spherical aberrations and defocus is that some features of the object have reversed contrast. Restoration of the image is partially possible; however, the operator should balance the contrast enhancement and the distortion of the object representation. In order to retrieve the true features of the object, the phase contrast transfer function (CTF) of the microscope must be corrected. CTF is a function intrinsic to a microscope and it modulates the amplitude and phase of the electron diffraction pattern formed on the back focal plane of the lens. CTF depends on several values, namely the spherical aberration coefficient, wavelength and defocus as illustrated in the following equation:

$$T(k) = -\left[\frac{\pi}{2} C_s \lambda^3 k^4 + \pi \Delta f \lambda k^2\right]$$

Where, C_s is the spherical aberration coefficient, λ, wavelength, Δf, defocus values, and k, the spatial frequency.

Correcting the CTF will eliminate its effects. CTF correction is accomplished by comparing and fitting the CTF curve to a model CTF (Zhou, Hardt et al. 1996).

Micrographs contain variations in contrast that represent density variation of the object; however, it also includes noise. In single-particle reconstruction, each image represents a projection of the object at a certain point of view. After image recording and processing, images must be aligned to extract three-dimensional information of the object – which means that the position and orientation of each particle must be identified so it can be superimposed with similar images. This is accomplished by the identification of

modifications (such as rotations or shifts) relative to a reference image. Usually, cross-correlation function (CCF) is used to compare two images and it is represented as

$$CCF(\vec{s}) = \frac{\int g_1(\vec{r} + \vec{s}) g_2(\vec{r}) \mathrm{d}\,\vec{r}}{\sqrt{\int g_1(\vec{r}) g_1(\vec{r}) d\vec{r} \times \int g_2(\vec{r}) g_2(\vec{r}) d\vec{r}}}$$

Where g1($\vec{r}$) and g2($\vec{r}$) are two functions, $\vec{r}$ is a vector in space, and $\vec{s}$ is the shift between images. Iteration is also important in this step since it gradually improves the reference image during refinement rounds (Orlova and Saibil 2011).

6. Aims of the Project

Members of the *Caliciviridade* family are very important pathogens of human and animals. The lack of an efficient propagation system is a major impediment to the study of human caliciviruses. Additionally, some studies suggest that cell attachment and entry appears to be the main block to efficient human calicivirus growth in cell culture. Further investigation of the early stages of the calicivirus infection is required in order to better understand host selectivity and to develop new culture systems. FCV, a common surrogate model for human caliciviruses, has been extensively studied. The mechanism of entry, however, is not completely understood. Previous data showed that FCV capsid undergoes a major conformational change upon binding with its physiological receptor, suggesting the initial steps of uncoating. The extent of this conformational change may only be understood by taking into consideration the endosomal low pH environment required for FCV infection. Although FCV replication is known to occur in membrane vesicles characteristic of positive-sense RNA virus, the mechanism of formation of these vesicles is still unknown. Understanding how FCV hijacks cellular systems would contribute to the development of vaccines and antivirals used in the prevention and treatment of calicivirus infection.

CryoEM, along with three-dimensional image reconstruction, have greatly contributed to the study of structural biology, and, in particular, to virus structure. However, the diversity and complexity of techniques involved in such procedures can generate misleading results. Further analysis of different reconstruction techniques will benefit the production of more reliable reconstructions.

The focus of this project was to elucidate the mechanism of cell entry for FCV, in particular, (1) the role of endosomal pH in conformational changes to the capsid and also (2) the process of uncoating. Also, (3) to use cryoEM and three-dimensional image reconstruction to understand how FCV-induced replication complexes relate structurally to each other and to organalles in the cell. To better assess the reconstruction techniques used in this project, we compared reconstructions of sapovirus-like particles calculated throught different procedures.

CHAPTER 2:

A structural comparison of sapovirus-like particles with other caliciviruses using cryo-electon microscopy and three-dimensional image reconstruction

1. Introduction

Due to the lack of efficient culture systems for caliciviruses, the mechanism by which viruses interact with host cells is poorly understood. Two surrogate models have been intensively studied to understand calicivirus infection, FCV and MNV (Guix, Asanaka et al. 2007). Atomic resolution structures of both virions and recombinant virus-like particles have been solved for several caliciviruses using cryo-electron microscopy and X-ray crystallography.

In recent years, VP1 of SV has been successfully expressed in insect cells, leading to the formation of empty virus-like particles that appear to be similar in structure to the native SV virion (Hansman, Ishida et al. 2007, Hansman, Oka et al. 2008). The structure of SV capsid, however, has not been described in great detail yet.

Herein, an icosahedral reconstruction of recombinant sapovirus-like particles generated by cryo-electron microscopy is described and compared with reconstructions of related caliciviruses. In addition, we compare reconstructions generated by different software. We show that SV-like particles exhibit the same general features of caliciviruses, with major differences present in the P2 domains, and resemble more closely the MNV structure rather than FCV.

2. Materials and Methods[1]

Viruses. Two strains of SV were isolated: SV Mc114 strain (GenBank no. AY237422) – recovered from an infant with acute gastroenteritis in Chiang Mai, Thailand, in 2001 (Hansman, Katayama et al. 2004) – and SV C12 strain (GenBank no. AY603425) – isolated from an infant with gastroenteritis in Sakai, Japan, in 2001 (Katayama, Miyoshi et al. 2004).

Cloning of viral cDNA to produce recombinant bacmids. SV consctructs used in recombinant VP1 (rVP1) expression contained (1) the VP1 gene from the predicted VP1 start AUG codon, (2) the VP2 gene and (3) polyadenylated sequences. Fragments were

[1] *Note: The production of recombinant sapovirus-like particles, cryo-electron microscopy and the three-dimensional reconstruction of one of the models presented here was carried out by David Taylor, from the National Institute for Physiological Sciences, Okazaki, Japan, and Grant Hansman, from the National Institute of Infectious Diseases, Tokyo, Japan. Such methods are only described here for the validity of the study.*

amplified by PCR and cloned according to the Baculovirus Expression system protocol (Invitrogen™ Life Technologies). The primers used for Mc114 strain were p+1Mc114 and attB2TX30SXN. For the amplification of the C12 strain, the primers used were the p+1C12 and attB2TX30SXN. After electroforesis, PCR fragments were cut out from the 0.8% agarose gel and purified. Fragments were cloned into a donor vector pDONR201 (Invitrogen™ Life Technologies) and subsequently transferred into a baculovirus transfer vector pDEST8 (Invitrogen™ Life Technologies). The recombinant pDEST8 was purified and used to transform DH10Baccompetent cells (Invitrogen™ Life Technologies) were transformed with pDEST8 producing recombinant bacmids containing the VP1 gene.

Expression in insect cells. Sf9 cells (Riken Cell Bank, Japan) were transfected with recombinant bacmids containing the VP1 gene; the resultant recombinant baculoviruses were collected as previously described (Hansman, Natori et al. 2005). Confluent Tn5 cells (Invitrogen™ Life Technologies) were infected at a multiplicity of infection (MOI) of 5-10 with the recombindant baculoviruses in 1.5 ml of Ex-Cell 405 medium (JRH Biosciences) followed by incubation at 26°C. 5 to 6 days post infection, culture medium was harvested and centrifuged for 10 min at 3,000×g, and further centrifuged for 30 min at 10,000×g. VLPs were concentrated by ultracentrifugation for 2h at 45,000 rpm at 4°C (Beckman TLA-55 rotor).

Electron Microscopy. VLPs were prepared for cryo-electron microscopy at a concentration of 1.0mg/ml, loaded onto a glow-discharged R1.2/1.3 Mo 200 mesh holey carbon grid (Quantifoil). Samples were blotted for 7/8 seconds and quickly punged into liquid ethane using an FEI MarkIV Vitrobot. Specimens were observed using a JEOL JEM-2200FFC microscope equipped with a field emis sion gun. Images of the samples were collected at a magnification of 80,000× using a charge-coupled-device camera, with a resulting sample size of 1.6Å/pixel.

Three-Dimensional Image Reconstruction. Two reconstructions of the VLPs were generated using different methods. To generate the first reconstruciton, David Taylor used the following methods: EMAN2 software was used to select and extract particles from micrographs; individual particles were normalized and phase flipped. A high-pass filter was applied prior to analysis; ~8,000 particle images were aligned and classified through multireference alignment and multivariate statistical analysis in IMAGIC (van Heel, Harauz et al. 1996); the initial model was generated in EMAN2, considering the best match

between reprojections, and further refinement was accomplished by sequential rounds of matching projections, cultimating in a 10Å resolution final reconstruction. Complementarily, we generated the second reconstruction using the micrographs recorded by David Taylor.. Images of VLPs particles were extracted and the contrast transfer function (CTF) was corrected using the BSOFT program BSHOW (Heymann 2001). Images were centered, oriented and reconstructed using PFT2/EM3DR2 (Baker and Cheng 1996). The generated FCV reconstruction was visualized using UCSF Chimera software (Pettersen, Goddard et al. 2004).

3. Results

Recombinant Sapporo virus-like particles exhibit common features of caliciviruses.

A three-dimensional reconstruction of SV-like particles (SVLPs) was generated from 2943 particles selected from a total of 222 micrographs (**Fig.2.1A**) recorded by David Taylor and provided by Grant Hansman. The final reconstruction has a calculated resolution of 9 Å.

Cryo-electron microscopy of SVLPs showed that SV-VP1 expressed in insect cells assembles into virion-like particles approximately 40nm in diameter (**Fig.2.1B**). SVLPs presented mainly with two different morphologies: (1) a well-defined organization, with a circular shell, clear protruding spikes arranged radially and extending from the shell, and a less dense interior (black arrows in **Fig.2.1B**); (2) a more disordered structure, with eccentric shells filled with a denser material inside (white arrows in **Fig.2.1B**).

As predicted, three-dimensional reconstruction of SVLPs showed 90 arch-like dimers of capsomeres (**Fig.2.1D**) arranged in a pattern consistent with T=3 icosahedral symmetry, similar to the other members of the *Caliciviridae* family. CC dimers, arranged at the 2-fold axes, and AB dimers, arranged around the 5-fold axes, present P2 domains pointing outwards from the centre of the particle (**Fig.2.1C**). A clipped view of the three-dimensional reconstruction cut to show the VLP interior, showed that SVLPs have no material inside the capsid (**Fig.2.1E**). The inner surface presents a series of organized features: the imprint of the 3 fold axis and a major indentation located at the 5fold axis (**Fig.2.1F**).

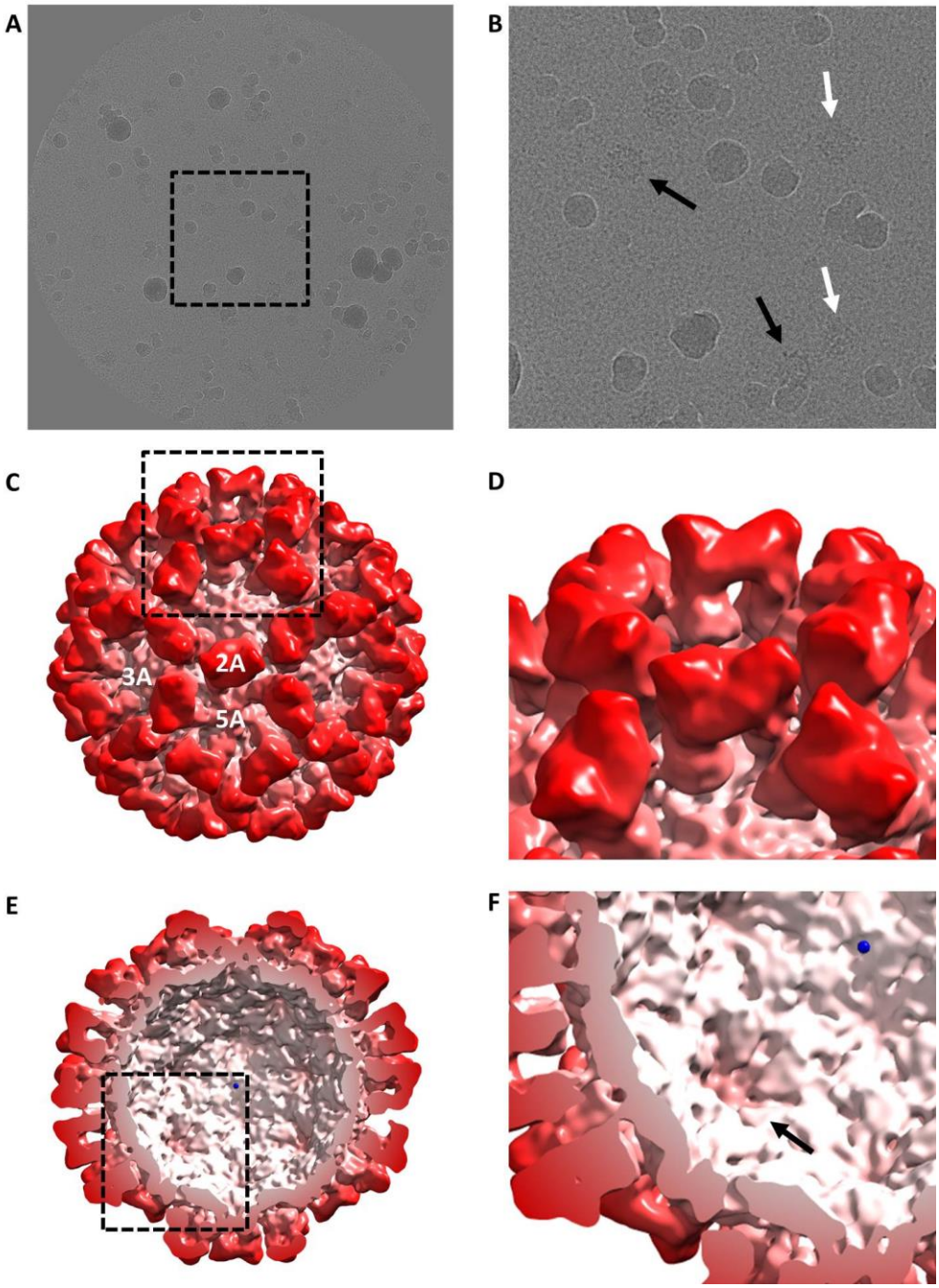

Figure 2.1 – **Cryo-EM visualization and three-dimensional reconstruction of SVLPs.** (A and B) SVLPs in cryoEM. B is the enlarged region highlighted in A. Black and white arrows point to SVLPs. Darker blobs found in the micrographs are likely to be contamination with condensed ice (C to F) SVLP three-dimensional image reconstruction. 2A: 2fold axis, 3A: 3fold axis, 5A: 5fold axis. (D) is the enlarged region highlighted in C. (E) Internal view of SVLP reconstruction. (F) is the enlarged region highlighted in E. black arrow: 5fold indentation.

SV-like particles are morphologically closer to murine norovirus than to feline calicivirus.

To compare the structures of SVLPs with two cultivable caliciviruses, SVLP three-dimensional reconstruction was overlapped and aligned with the published structures of FCV and MNV.

Major differences between SVLP and FCV three-dimensional reconstructions are found in the P2 domains of dimers (**Fig.2.2A**). FCV dimers have more flat, rhomboid protruding domains contrasting with the slender and spikier tops of the SVLP capsomeres. Minor differences are also observed in the S and P1 domains.

In comparison to MNV three-dimensional reconstruction, dimer arrangements are very similar and elongated P2 domains are observed in both species (**Fig.2.2C**). MNV P2 domains are located in the uppermost part of the top of the dimer, as observed in SVLP, however they appear to be rotated by 41° in relation to SVP P2 domains (**Fig.2.2C**).

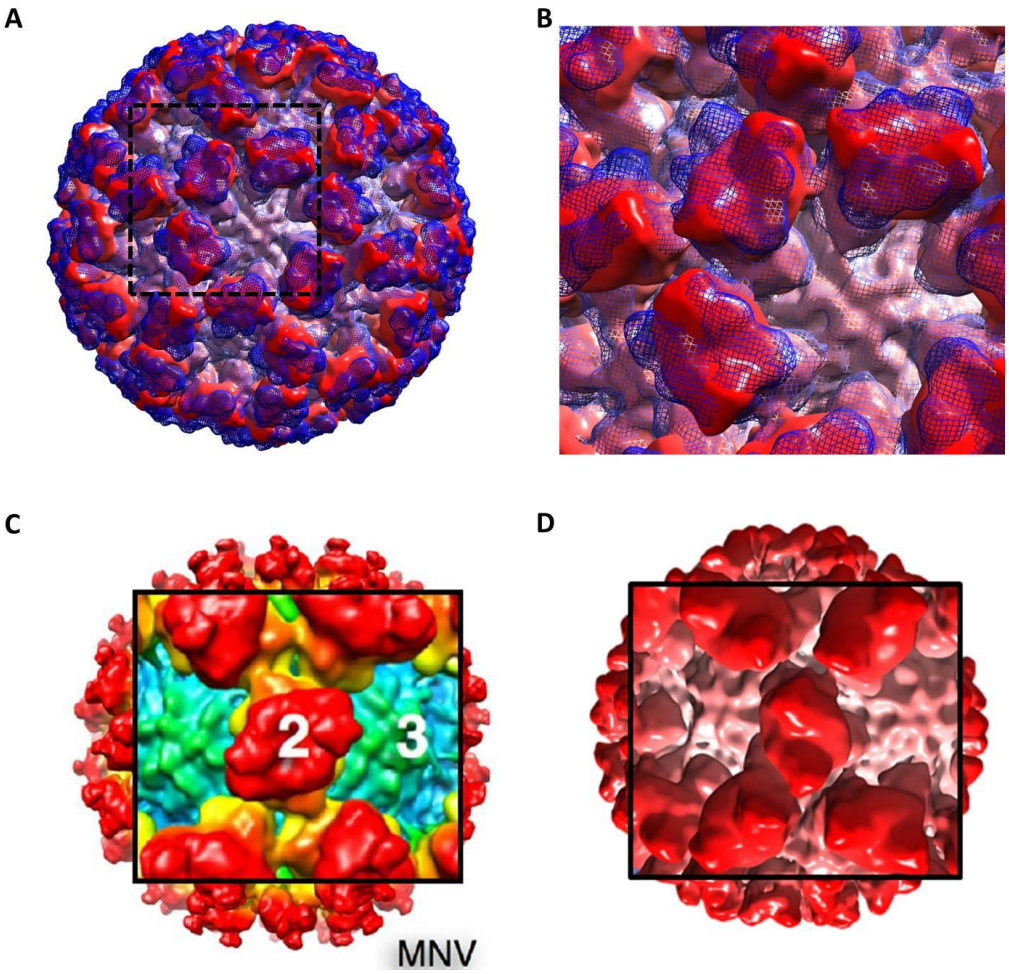

Figure 2.2 - **Comparison of SVLP Reconstruction with other caliciviruses**. (A) FCV and SVLP maps merged. (B) enlargement of boxed region in A. (C) Detail of MNV reconstruction. (D). Detail of SVLP reconstruction

Application of different software approaches to 3D reconstruction can lead to different outcomes.

To analyze the influence of reconstruction software on alignment and 3D reconstruction of a dataset and the consequences for the final outcome, two reconstructions of the same data set were obtained using different three-dimensional reconstruction techniques. The first reconstruction was accomplished by Hansman *et al.* (unpublished data) using EMAN – a software package for single-particle reconstruction from transmission electron micrographs developed in 1999 by Ludtke *et al.* in Baylor College of Medicine, Texas; the second reconstruction, calculated for this project, was generated as described previously in the Materials and Methods section.

In Hansman's reconstruction (**Fig.2.3A**), P domains of VP1 dimers appear to have higher resolution as evidenced by finer features in the iso-surface representation of the map. The shell domain appears however the characteristic arch-like structure is less easily seen at this threshold level compared to our reconstruction, which was calculated using PFT2/EM3DR2 (**Fig.2.3B**). Floating around the structure, ten non-symmetric aggregates are shown aligned with the 5-fold axes and in close proximity of the capsid (black arrows in **Fig.2.3A**). These densities are caused by symmetrized noise being integrated into the reconstruction. Interestingly, when a clipped view is applied to the reconstruction, the interior is filled with a disorganized material with a denser layer located next to the inner surface of the capsid (black arrow in **Fig.2.3C**). Such material is not displayed in our reconstruction (**Fig.2.3D**).

A critical difference between these two reconstructions in addition to the method of 3D reconstruction is the application of B-factor correction to suppress low-resolution features. The B-factor correction is a processing technique that down-weights the low-resolution terms that otherwise would dominate the map. This was applied to the map calculated by Hansman *et al.* but not to ours in the first instance. To make a direct comparison, B-factor correction was applied to our map using the EM B-factor program (Fernández, Luque et al. 2008) (**Fig.2.4A** and **B**). This map showed comparable high-resolution features to those seen in Hansman's structure. Moreover, in this map the AB and CC dimers show more consistent features.

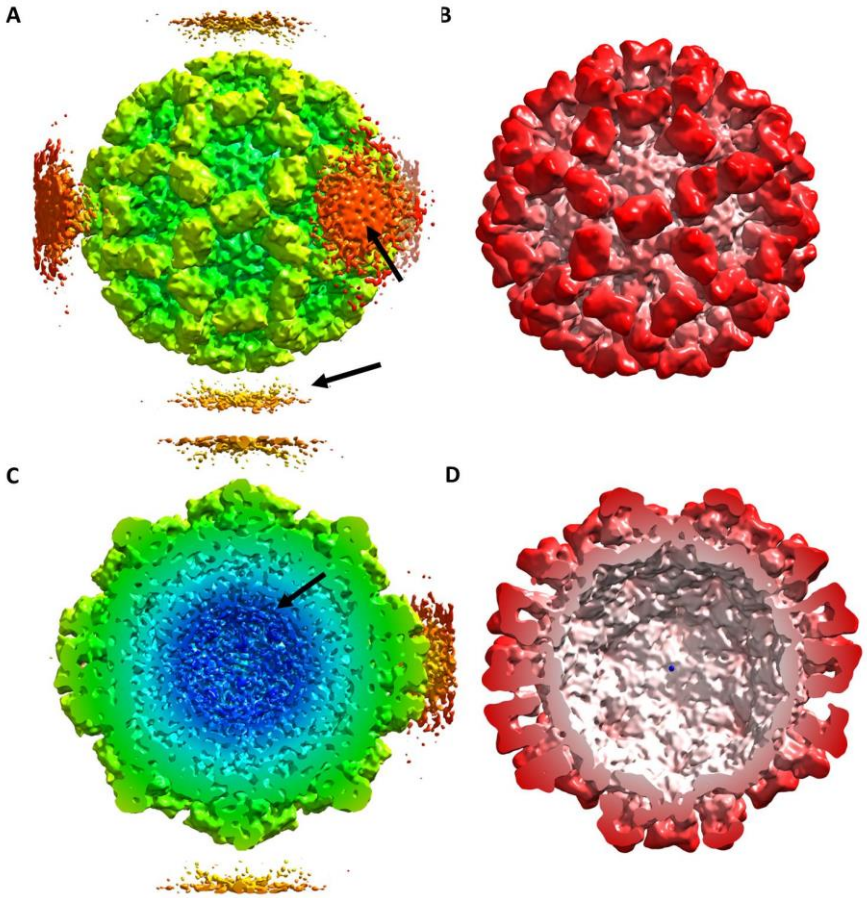

Figure 2.3 - Comparison the SVLP reconstructions generated by EMAN (A, integral, and C, side view) and EM3DR2 (B, integral, and D, side view)

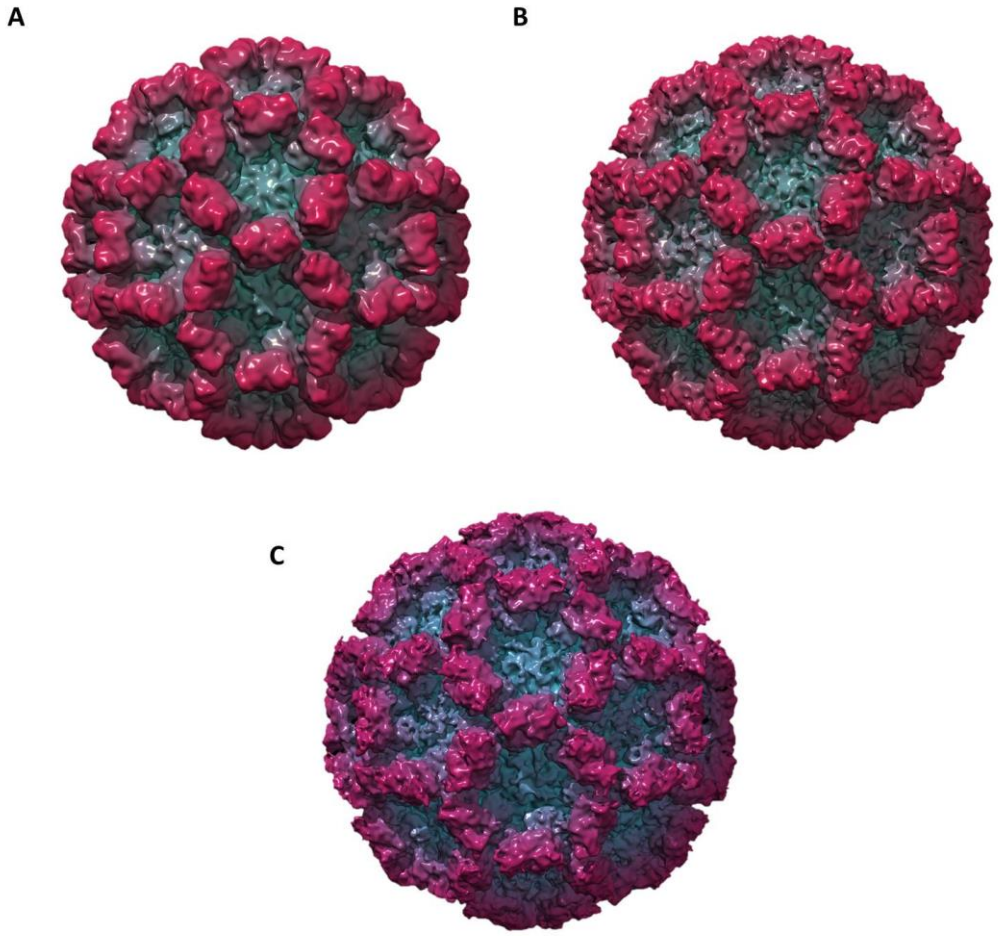

Figure 2.4 – Application of B-factor correction to the different reconstructions of SVLPs. (A) SVLP reconstruction generated by EM3DR2 and (B) with the B-factor correction. (C) SVLP reconstruction using EMAN.

4. Discussion

In the present study, the structure of recombinant sapovirus-like particles has been determined using cryo-electron microscopy and three-dimensional image reconstruction, being the first study to show the structure of a recombinant human sapovirus VP1 in a VLP assembly. We have shown that SVLPs present most of the features of the *Caliciviridae* family with major differences centred in the P2 domain. Furthermore, we have compared the influence of reconstruction strategy in single-particle reconstruction software and its effects in interpreting the final reconstruction.

Our data suggests that amongst the *Calicivirdae* the P2 domain is the most variable region in VP1, supporting the hypothesis that the P2 domain is the most important region for host permissivity and antigenic variation. The similarities found in the

organization of P2 domains between sapovirus and MNV pinpoints the latter as a better surrogate model for sapovirus studies than to FCV. Although studies show MNV replication is enteric and leads to infection only in immunocompromised mice, with broader symptomatology than human noro- and sapoviruses, MNV does not produce clinical symptoms in wild-type mice. Major significant structural differences in SVLPs and MNV are focused on the orientation of the P domains of dimers relative to the S domain. We hypothesized that this shift in the orientation of the P domains between species of different genera may be an important factor for receptor binding, as rotation of the P domain has been shown to occur upon receptor binding (Bhella and Goodfellow 2011). Since all the receptors identified so far for caliciviruses are protein members of the histo-blood compatibility group, it is fair to admit that the organization of these molecules in cell surface between different hosts and different cell types would a limiting factor for virus propagation in cell culture. Therefore, the study of structural organization of caliciviruses is essential to understand the limitations of *in vitro* cell systems and develop new ways to approach and overcome this problem.

Studies on virus structure depend deeply on electron microscopy and image reconstruction software. It is critical then to perfect and validate the software and approaches used to generate 3D reconstruction. Moreover, it is important to judge the quality of reconstruction both qualitatively and quantitatively, since it does not absolutely define the resolution achieved in a study if overfitting is not adequately controlled (Cohen 2013, Mao, Wang et al. 2013). In this study we compared two different software packages by generating SVLP reconstructions: EMAN and EM3DR2. As described previously, the structure of SVLP generated by EMAN showed an amplification of noise in the micrographs, generating random and disorder structures above and inside the capsid. Such structures are not represented in EM3DR2's reconstruction. Such differences can be due to a possible defective filtering in EMAN or low contrast threshold. P2 domains, initially, appeared to be better resolved in the reconstruction using EMAN, this was found to be a consequence of the B-factor compensation that was applied. When a similar correction was applied to our map, similar high-resolution features emerged, however our map had AB and CC dimers that were more self-consistent.

CHAPTER 3

A study of feline calicivirus conformational changes in low-pH environment

1. Introduction

FCV structure has been determined by cryoEM and X-ray crystallography studies, showing that its capsid is comprised of 180 copies of VP1, the major capsid protein, forming 90 arch-like dimers arranged in a T=3 icosahedral lattice. VP1 can thus assume three different conformations, known as A, B, and C, generating two classes of dimers: AB dimers, arranged around the 5fold symmetry axes, and the CC located at the 2fold symmetry axes (Prasad, Matson et al. 1994, Prasad, Hardy et al. 1999).

The cellular receptor for FCV has been determined: fJAM-A binds to FCV, soluble forms neutralize the virus, and transfection of non-permissive cells with the fJAM-A gene renders them susceptible to infection by virus (Makino, Shimojima et al. 2006, Pesavento, Chang et al. 2008). Studies of soluble fJAM-A bound to FCV have shown that the capsid undergoes major conformational changes leading to the loss of the icosahedral symmetry. It has been hypothesized that theses conformational changes may represent the initial steps of the uncoating and penetration process (Bhella, Gatherer et al. 2008, Bhella and Goodfellow 2011).

After receptor recognition, FCV enters the cell by clathrin-mediated endocytosis (Stuart & Brown, 2006). The virion is endocytosed into a vesicle coated with clathrin; subsequently clathrin dissociates and the vesicle fuses with an early endosome. At later stages in the pathway, the particle is transported to the late endosome. At some point the virus particle penetrates the membrane of the endosome, escaping or exporting its genome to the cytosol (Smith et al. 2004). Studies in endosomal acidification inhibition with chloroquine showed that a low-pH step is required for a successful FCV infection (Kreutz et al. 1995, Stuart et al. 2004). Kreutz et al. identified this critical step up to 2h after virus adsorption.

In this study, we attempted to determine the structure of FCV bound to fJAM-A in a low-pH environment and analyze the conformational changes associated to this step.

2. Materials and Methods

Viruses culture and purification. Feline calicivirus strain F9 was propagated in FEA and CRFK cells (kindly provided by Dr. Brian Willett, Faculty of Veterinary Medicine, University of Glasgow, Scotland, United Kingdom) in Dubecco's Modified Eagle's medium (DMEM - Gibco® Life Technologies) supplemented with 10% Fetal Bovine Serum (Gibco® Invitrogen) and 1% Penicillin Streptomycin (100 U/ml penicillin, 100 ug/ml streptomycin, Gibco® Life Technologies), using a multiplicity of infection (MOI) of 0.1 or 0.01. Cells were

lysed by a single freeze-thaw, and the supernatant was clarified by centrifugation (4000rpm, 30min at 4°C, Thermo Scientific® Heraeus Megafuge40R centrifuge) and then filtered through a 0.45µm filter (Minisart® Sartorius). Virus particles were precipitated by the addition of solid polyethylene glycol (PEG) with a molecular weight of 3,350 (Sigma®) to a concentration of 10%(w/v) and sodium chloride (0.2 M, AnalaR Normapur®). After 14, 17, and 20 hours incubation at 4°C, precipitated virus was recovered by centrifugation (11500rpm/17948×g, 30min at 4°C, Thermo Scientific® Sorvall Centrifuge Rotor SureSpin 630) and resuspended in 0.2 M boric acid buffer (Normapur®, pH 7.4, in Dulbecco's Phosphate Buffered Saline 1x Sigma®) containing 0.5 M sodium chloride (AnalaR Normapur®), for different periods of time (1, 2 and 3 hours). Insoluble material was removed by centrifugation (11500rpm/17948×g, 30min at 4°C, Thermo Scientific® Sorvall Centrifuge Rotor SureSpin 630), and virus particles were partially purified by centrifugation through a 30%(w/v) sucrose cushion (Sigma®) at 24600rpm/112398×g for 15h at 4°C. The virus pellet was resuspended in phosphate-buffered saline and banded in an isopycnic cesium chloride gradient (1.31 g/ml, Melford®) by centrifugation at 40200rpm for 20 h at 4°C (Thermo Scientific® Sorvall Centrifuge Rotor AH-650). Virus was removed from the gradient, dialyzed against phosphate-buffered saline, and subsequently concentrated using a 100-kDa-molecular-mass-cutoffcentrifugal concentrator (Vivaspin 4 Sartorius). Other FCV preparation held in stock was also used and was prepared as described previously (Bhella, Gatherer et al. 2008).

Virus Titration. To access the cell culture infectious dose 50% (CCID50) of FCV in FEA and CRFK cells, virus titrations were carried out in 96 well plates. Initially, 10µl of the sample was diluted into 5ml of DMEM, followed by a sequential dilution of 1:2000, 1:8000, 1:32000, 1:128000, 1:512000, 1:2048000, 1:8192000, and 1:3276800, in quadruplicates. FEA or CRFK cells were seeded in each well to a final concentration of $2x10^5$ cells/ml. Plates were then incubated at 37°C and examined post infection.

Electron Microscopy. Purified FCV was incubated in the presence of soluble fJAM-A (kindly provided by Dr. Ian Goodfellow, Department of Virology, Faculty of Medicine, Imperial College London) for 1h at 4°C. The pH of virus containing solution was modified by the addition of a 100m citrate phosphate buffer (Citric Acid, Sodium Phosphate AnalaR®, pH=5;5.5;6) for 5 or 30min at 4 or 37°C. FCV particles were prepared for cryo-electron microscopy: glow-discharged (Emitech-K100X) C-flat™ holey

carbon grids (CF-22-4C, Protochips®) were covered with 4µl of FCV particles in PBS. Grids were blotted for a few seconds and then plunged into liquid ethane kept cold by liquid nitrogen. Frozen FCV-covered grids were observed at low temperature in a JEOL 2200 FS Cryomicroscope equipped with a Gatan 626 cryo-stage. Samples were imaged at a magnification of 100,000×.

Negative-staining electron microscopy was also used for rapid evaluation identification of FCV virions at certain stages during the purification procedure. Prior to the staining, square mesh grids (AGG2400C Square 400 Mesh Copper 3.05mm, Agar Scientific, Ltd.) were coated with a thin Formvar film (Agar Scientific, Ltd.). A uniform carbon layer was deposited onto the Formvar film using a Quorum Q150T Carbon Coater with a ramping current of 40A. Formvar was then dissolved using a chloroform solution (VWR Prolabo 0,6% ethanol). 4µL aliquots of FCV samples were loaded onto freshly glow-discharged carbon-coated grids. The grids were washed three times in deionized water and finally stained in an ammonium molybdate solution (2% pH=7, Agar Scientific, Ltd.) and air dried. Negative stained samples were imaged in a JEOL 1200 EXII electron transmission microscope.

Three-dimensional image reconstruction. To calculate reconstructions, 223 micrographs of FCV strain F9 virions were processed. Micrographs were binned by a factor of two, giving a sample frequency of 2.06 Å/pixel. Images of FCV particles (1944 in total) were extracted and the CTF was corrected using the BSOFT program BSHOW (Heymann 2001). Images were centered, oriented and reconstructed using the EM3DR2 program (Baker and Cheng 1996). The generated FCV reconstruction was calculated from 1745 particles and visualized using UCSF Chimera software (Pettersen, Goddard et al. 2004).

3. Results

FCV-fJAM-A microscopic structure is significantly affected by low pH environment

Purified FCV virions were allowed to bind to soluble fJAM-A as described previously, generating FCV virions decorated with fJAM-A. The pH environment was changed after initial decoration with the receptor and particles were observed by cryo-electron microscopy (**Fig.3.1**)

Micrographs of FCV-fJAM-A complexes in different pH environments showed that particles undergo a substantial structural change. At neutral pH (pH=7.0), fJAM-decorated FCV particles display a concentric shell with distinctive VP1-fJAM protrusion, measuring about 50nm in diameter (**Fig.3.1A**). At pH 5.5 and 5 (**Fig.3.1B** and **3.1C**, respectively) particles show a smaller diameter, 30nm approximately, with a disordered exterior. The shell line is no longer recognized, suggesting that the particles collapsed into the centre of the virion but maintained a morphology that still resembles virus particles.

To investigate this structural change, data were collected with the intention of processing particle images to calculate a three-dimensional image reconstruction. This aim was hampered by a persistent aggregation of virus particles that was found in all FCV samples (**Fig.3.1D**). In cryo-electron microscopy, aggregation and overlapping of virus particles usually obscures features of the particles and they can not be used for a reliable three-dimensional image reconstruction. Consequently we decided to work towards identifying an FCV preparation suitable for microscopy studies.

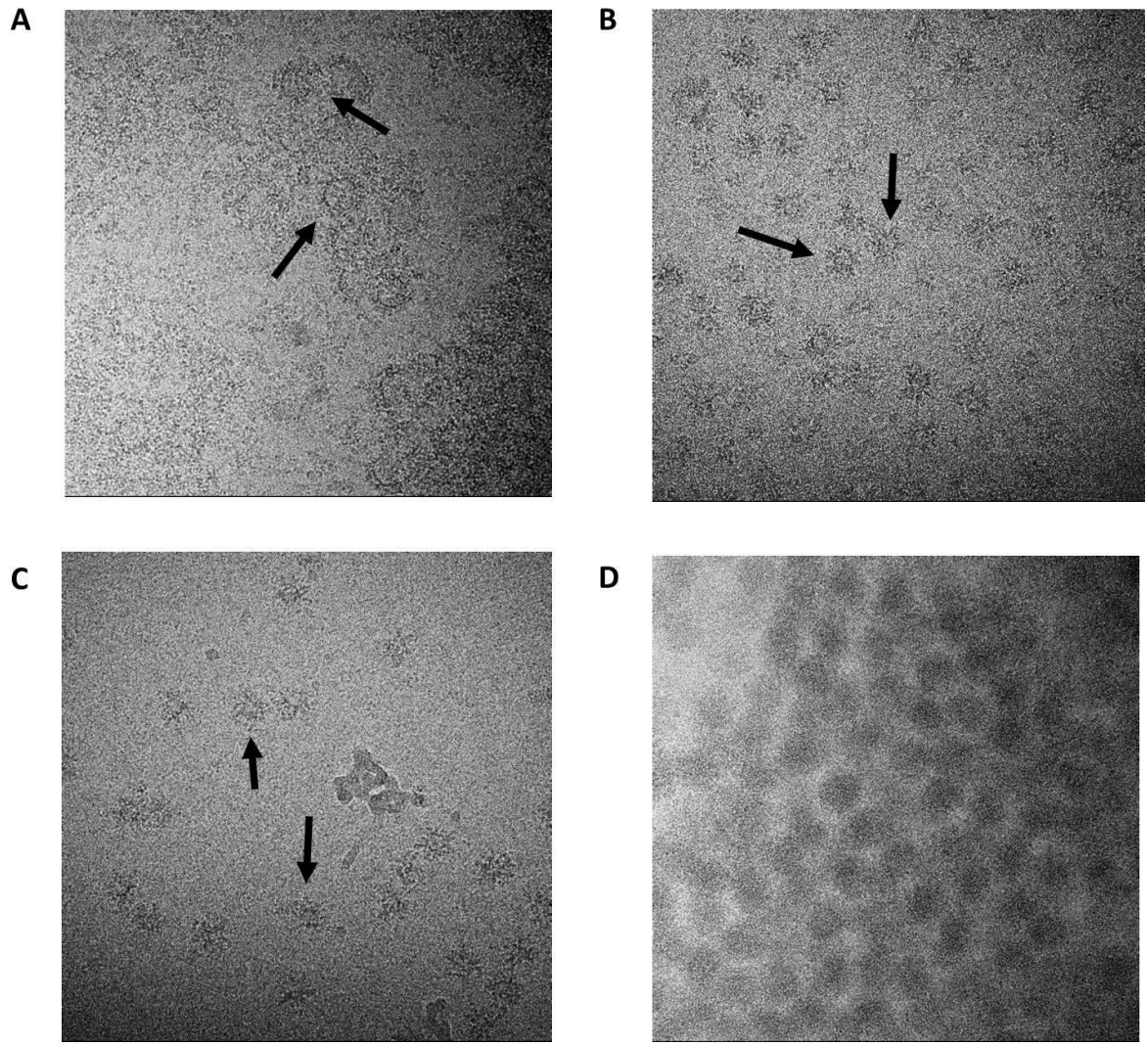

Figure 3.1 - FCV-fJAM-A cryoEM micrographs 100,000X at low pH. (A) FCV particles bound to soluble fJAM-A in neutral pH showing a rounder structure, (B) FCV-fJAM-A complexes in pH 5.5, and (C) in pH 5. Black arrows in images A, B, and C point to FCV virions labeled with fJAM-A. (D) FCV-fJAM-A complexes aggregated in pH 5.

Preliminary cryo-electron microscopy and three-dimensional reconstruction studies were performed to assess the viability of another FCV preparation held in stock in the laboratory. Cryo-electron microscopy studies of FCV virions showed that particles were well separated from each other, presenting the distinctive features of calicivirus morphology (**Fig.3.2A**).

A three-dimensional reconstruction of FCV was generated from 1745 particles selected from a total of 223 micrographs. The final reconstruction has a calculated

resolution of 13Å (**Fig.3.2B**). This structure showed similar features of those previously described but high resolution features were not well resolved, suggesting that the particles were not well preserved. Such a preparation would not allow the study of conformational changes upon fJAM binding and low-pH environment.

To overcome this problem, we decided to propagate FCV in cell culture and attempt to optimize the purification process.

FCV propagation in FEA cells

FCV was propagated in FEA cells using an MOI of 0.1 and 0.01 and virus titrations were performed for a period of 72 hours post-infection to optimize the conditions of virus replication and purification (**Fig.3.3**). It was observed that the most efficient MOI was 0.1 at 36/48h post-infection. This was the time used for further FCV purification.

The cytopathic effect caused by FCV in FEA cells was also observed during the titration (**Fig.3.4**). A confluent layer of FEA cells (**Fig.3.4A**) was cultivated as described in the Materials and Methods sections. FEA cells showed the first signs of FCV infection at 6/9h post-infection, at which time some cells had started to detach from the surface and become rounded. At 48 hours after infection, 50-60% of the cells were detached and were seen to be aggregated in small clusters that floated above the monolayer (**Fig.3.4C**). It was also observed that cellular debris was present in the aggregates. At this point, the culture medium

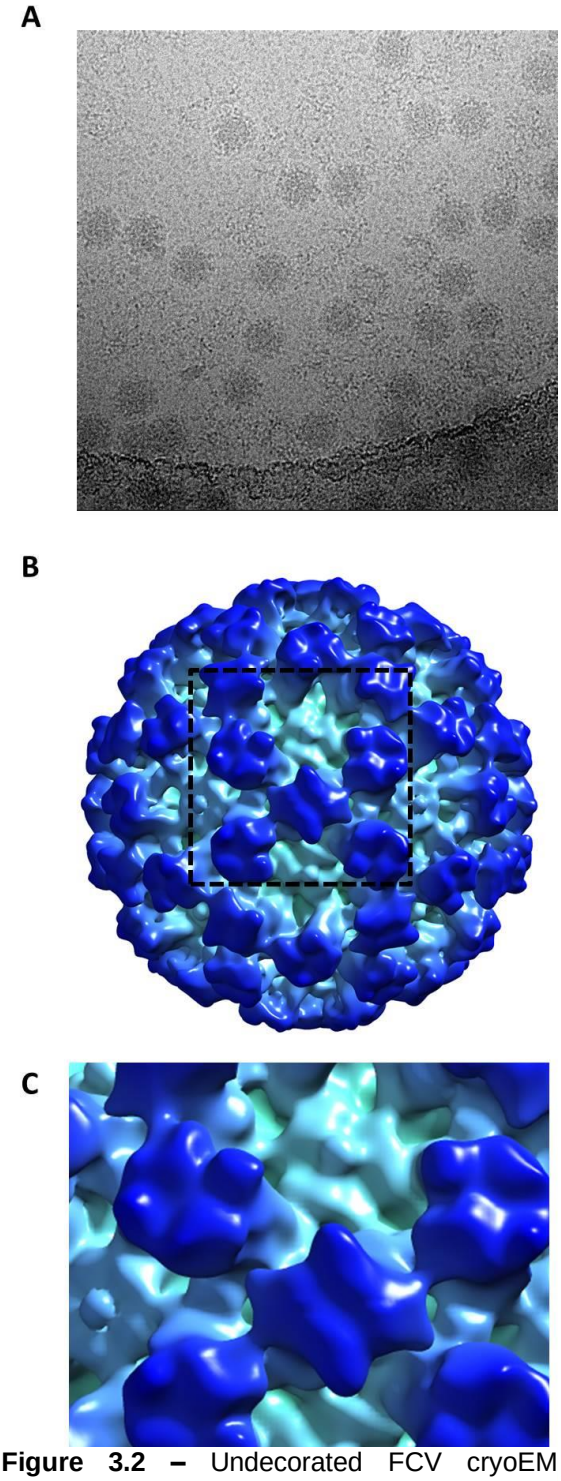

Figure 3.2 – Undecorated FCV cryoEM micrographs 100,000X (A). Three-dimensional representation of FCV reconstruction (B). Detail of representation of FCV reconstruction (C)

turned yellow indicating that pH had fallen below 6.8. Finally, at 72 hours post-infection, almost all the cells lost adhesion to the surface and cellular debris was observed throughout the plate (**Fig.3.4D**).

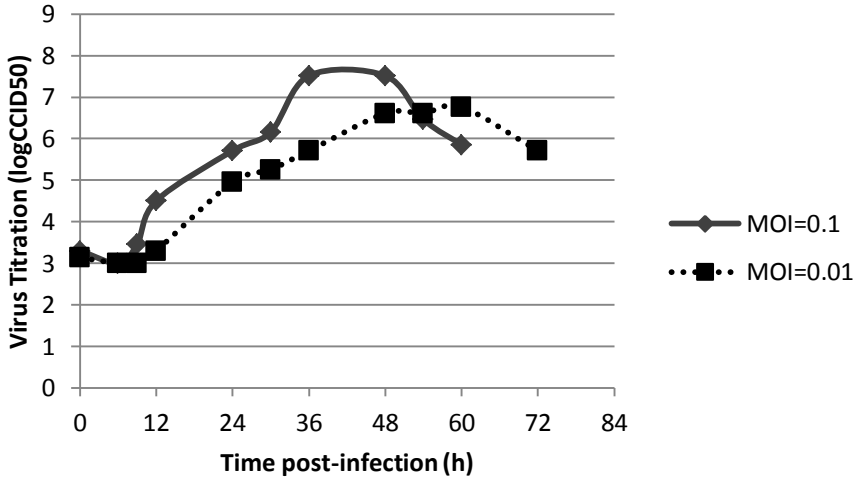

Figure 3.3 - FCV titration using FEA cells. Virus growth curves were used to evaluate the infection profile of FCV using different MOIs.

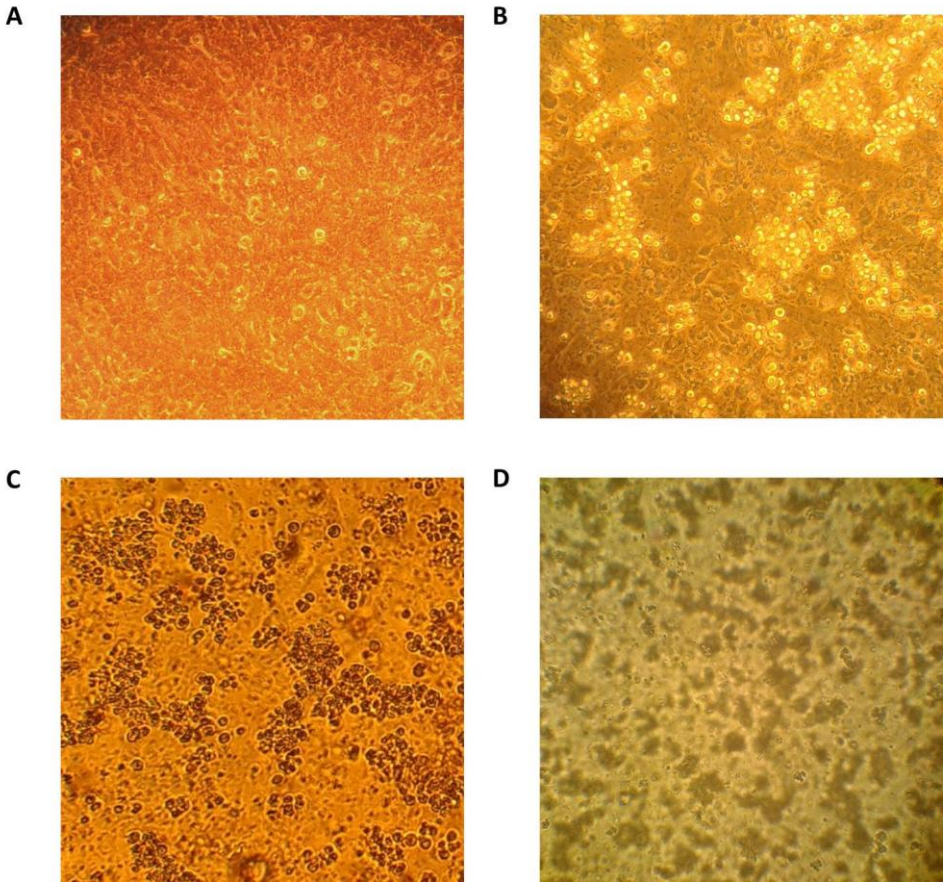

Figure 3.4 – Evolution of FCV cytopathic effect in FEA cells using optical microscopy. A confluent monolayer of FEA cells (A) was infected with FCV at an MOI of 0.1. Infection was followed up during 72 hours, and cell rounding and surface detachment was observed in infected cells at (B) 24h post-infection, (C) 48h, (D) and 72h.

FCV purification

After propagation in cell culture, FCV was collected at 40h post-infection and purified as described in the Materials and Methods sections. The purification process was modified several times, with the aim of improving yields. Initially, we focused on the PEG precipitation step since the amount of virus particles observed after this step decreased significantly. We tried different times for the PEG precipitation at 4°C: 14, 17, and 20 hours in a continuously stirred environment. No significant change was observed in the number of virus in samples at different periods of time. Then, we tried two different centrifugation speeds: 11.500 rpm and 15.000 rpm (**Fig.3.5**). We conclude that both conditions resulted in similar numbers of virions being seen by EM, although an increased amount of cellular debris was observed following centrifugation at 15.000 rpm. After the PEG precipitation

step and centrifugation, pellets were resuspended in a boric acid buffer. Boric acid dissolves PEG and releases virions into the supernatant. We hypothesized that the boric acid buffer might not be dissolving PEG appropriately. To test this, we performed experiments in which PEG was dissolved in boric acid on ice for different periods of time: 1, 2, and 3 hours (**Fig.3.6**). EM studies of these samples showed that the best time for PEG-boric acid dissolution is 2 hours in ice.

The next step of the purification protocol for FCV was centrifugation through a 30% sucrose cushion. In this procedure, 13.5ml of virus solution was placed on a 25ml sucrose cushion and centrifuged overnight at 25,000 rpm. After centrifugation, both pellet and supernatant were observed by EM to evaluate the numbers of virus particles. None of the samples showed the presence of FCV. We hypothesized that FCV particles might be disrupted during the 14 hour centrifugation. To test this we centrifuged 13.5 ml of virus suspension on to 5ml sucrose cushion for 2 and 3 hours. In both cases, however, virus particles were not observed in EM.

Caesium chloride gradients were also introduced into the purification protocol. Two bands were identified under polarized light located 3,5cm and 1cm down from the top of the tube. These bands were collected and observed in EM. No FCV particles were identified however.

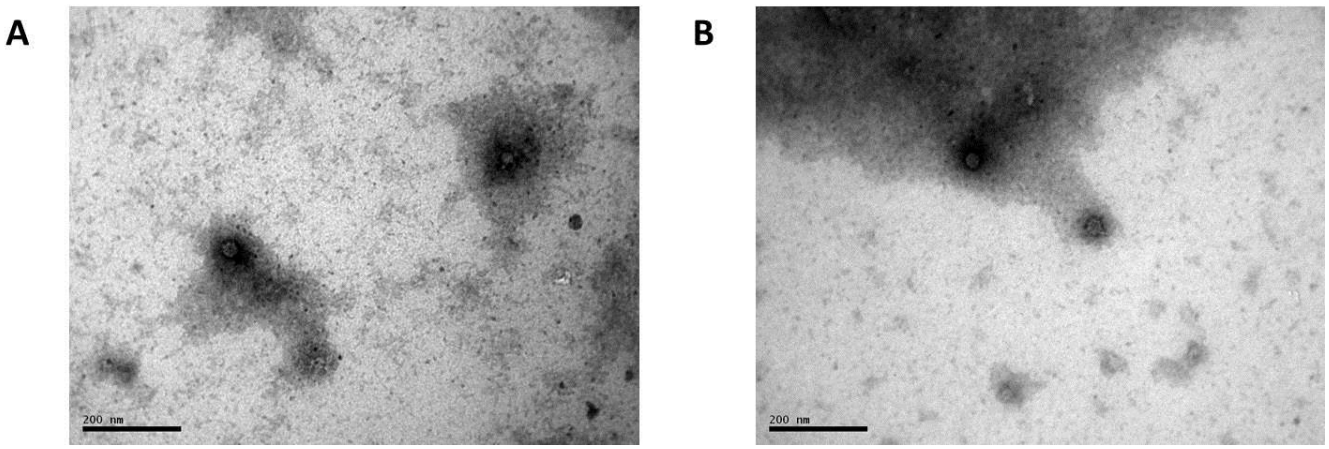

Figure 3.5 - Negative-stained FCV after PEG precipitation in EM. Both samples using 11,500 rpm (A) and 15,000 rpm (B) showed similar numbers of virions, with an increased amount of cellular after centrifugation at 15,000 rmp.

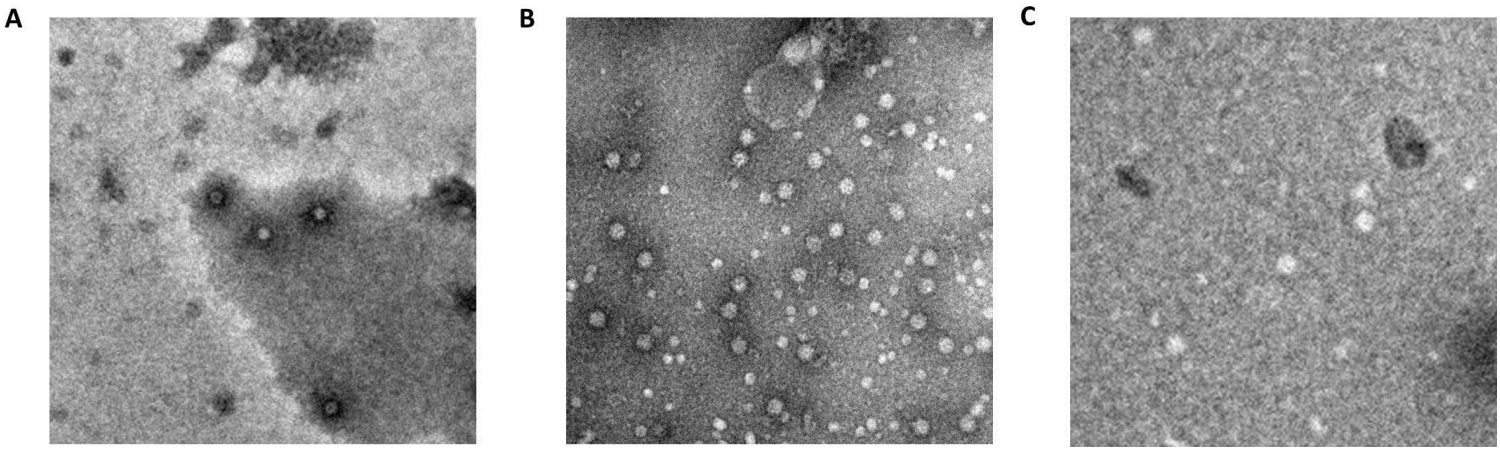

Figure 3.6 - Negative-stained FCV after PEG precipitation and boric acid buffer dissolution. FCV-containing pellets were allowed to react with boric acid buffer for (A) 1h, (B) 2h, (C) and 3h. A greater number of virions were observed after 2h of dissolution with boric acid buffer.

4. Discussion

Herein, we described a preliminary study of the conformational changes that FCV bound to fJAM undergoes in a low-pH environment. Our data suggests that a significant modification of FCV structure and size occurs in low-pH. A study on the mechanical properties of norovirus capsids showed that the shrinkage of the capsid occurs in acidic pH (Cuellar *et al.*, 2010). Although this study was not performed a using receptor-bound form of caliciviruses, this data suggests that low-pH shrinkage of the capsid might occur in physiological conditions. Some studies on positive-sense RNA viruses indicate that the genome is essential for adequate assembly of the capsid (Permutter *et al.,* 2013; Stockley *et al.,* 2013). We hypothesize that the radical conformational change observed in our study might be due to a release of the viral genome, leading to a loss of capsid integrity and an altered structure. In poliovirus, the rotation of some domains of the capsomers occurs upon membrane penetration and genome escape (Bubeck *et al.,* 2005; Hogle *et al.,* 2013). In our experiment, we used virions that were entirely coated with fJAM molecules and were exposed to low pH, the combination of which appears to have caused dramatic conformational changes.

Further microscopy studies should be performed to investigate these conformational changes in greater detail. Unfortunately the purification protocol employed in to this study failed to generate a sufficiently high quality FCV preparation to allow cryo-electron microscopy and three-dimensional image reconstruction within the time available. However, several optimizations were applied to this procedure and are described. The disappearance of FCV particles after sucrose cushion centrifugation might be attributed to a possible collapse of the capsid. Low speed centrifugation could be applied to this process, as well as an optimization of sucrose cushion height and density. In previous studies, a 30% sucrose cushion has been shown effective in isolating FCV particles. However, other methods exist that may prove superior such as replacing the centrifugation trichlorotrifluoroethane extraction this method was shown to give good quality preparations of FCV suitable for X-ray crystallography (Ossiboff *et al.,* 2010).

CHAPTER 4

Feline calivirus replication complexes are closely associated with endoplasmic reticulum

1. Introduction

Virus cell entry is usually mediated by receptor-binding and, in order to replicate, viruses must hijack cell machinery to synthesize their genome, capsid and other essential proteins. Some other positive-sense RNA viruses replicate their genomes in the cytoplasm, leading to the formation of small vesicles where viral RNA synthesis occurs (Egger and Bienz 2002, den Boon and Ahlquist 2010). FCV infection has shown the formation of small membrane-bound vesicles occurs and these vesicles are enzymatically active, containing all the units required for RNA replication (Green, Mory et al. 2002). However, little is known about the formation of these vesicles, how they relate to each other and from which organelle they originate.

In this study, we observed resin embedded FCV infected cells using TEM and three dimensional image reconstruction software to determine the relationship between FCV induced vesicles and the organelles in the cell.

2. Materials and Methods

Viruses culture. FEA cells were maintained in DMEM (Gibco® Life Technologies) supplemented with 10% Fetal Bovine Serum (Gibco® Invitrogen) and 1% Penicillin Streptomycin. FCV at an MOI of 10 was adsorbed to an 80% confluent FEA monolayer. A non-infected (mock-infected) FEA control was prepared in which the same procedure was followed in the absence of virus. Growth medium was removed 6, 9, and 12h after infection and cells were prepared for microscopy.

Resin Embedding. Cells were washed with PBS and fixed with cold glutaraldehyde fix (2.5% in PBS, TAAB Laboratories Equipment, Ltd.) for 1h at 4°C. After fixation, glutaraldehyde was removed and cells were washed with PBS. A 1% osmium tetroxide solution was added to the cells, incubating at room temperature for 1h. Osmium tetroxide was removed and cells were again washed in water. Samples were stained with a 2% uranyl acetate in water (AnalaR) at room temperature for 45min. Cells were scraped into water and pelleted at low-speed centrifugation. A 2% LGT agarose solution was incorporated into the cells, pelleted, and solidified on ice for 45min. The cell pellet was cut away from the rest of the agar and dehydrated with a series of ethanol solutions (Fisher Scientific UK, Ltd). Samples were infiltrated with a TAAB 812 Resin (TAAB Laboratories Equipment, Ltd.) and left at 65°C for two days.

Electron Microscopy. Resin embedded samples were prepared for electron microscopy. Sections of the embedded cells were cut using a Leica EM UC6 microtome, equipped with a 45° diamond knife (DiATOME). Sections were directly absorbed into G200Hex-C3 Ø3.05mm Copper Grids (Gilder Grids) and photographed on a JEOL 1200 EXII transmission electron microscope. Tomographic series of the samples were collected using a tilt range of 120° ($\pm 60°$) in a JEOL 2200 FS Cryomicroscope equipped with Gatan 626 specimen rod.

Three-dimensional image reconstruction. Tomograms were calculated by using etomo in the IMOD software package. Subtomograms were analyzed by using Amira (Visage Imaging GmbH, Berlin, Germany). A bilateral filter was applied to tomograms and contrast invert using SPIDER technology (System for Processing Image Data from Electron Microscopy and Related fields, Wadsworth Centre, Albany, New York, USA) The reconstructions were then segmented into interior and membrane regions.

3. Results

FCV infected cells show several characteristic features of positive-sense RNA virus infection.

FCV-infected and mock-infected FEA cells were embedded in resin, sectioned and observed in TEM. FCV-infected cells showed typical signs of pathology at 9 and 12 hours post-infection. Mock-infected cells are generally presented in an elongated shape, displaying a bold and regular nuclear outline and homogeneous chromatin density, with a highly organized cytoplasm (**Fig4.1.A**). On the other hand, FCV-infected cells presented with a rounder shape, with an uneven nuclear outline and irregular morphology – in some cases the nuclear envelope appears broken or fragmented, with protrusions of nuclear material into the cytoplasm, and fragmented. The cytoplasm is often more disordered with swollen organelles (**Fig.4.1B**).

Virus particles were only observed in FCV-infected cells. FCV virions were mainly observed in three different arrangements: small non-crystaline clusters, paracrystaline arrays (arrow in **Fig.4.1C**), and in association with membranes (arrow in **Fig.4.1D**). Virus particles often appeared to be associated with the vesicles, and their number per cell increased relative to the durantion infection. In later stages of infection, virus appeared to be packed in unusual cisternae and again in close association to the membrane (**Fig.4.1E and F**).

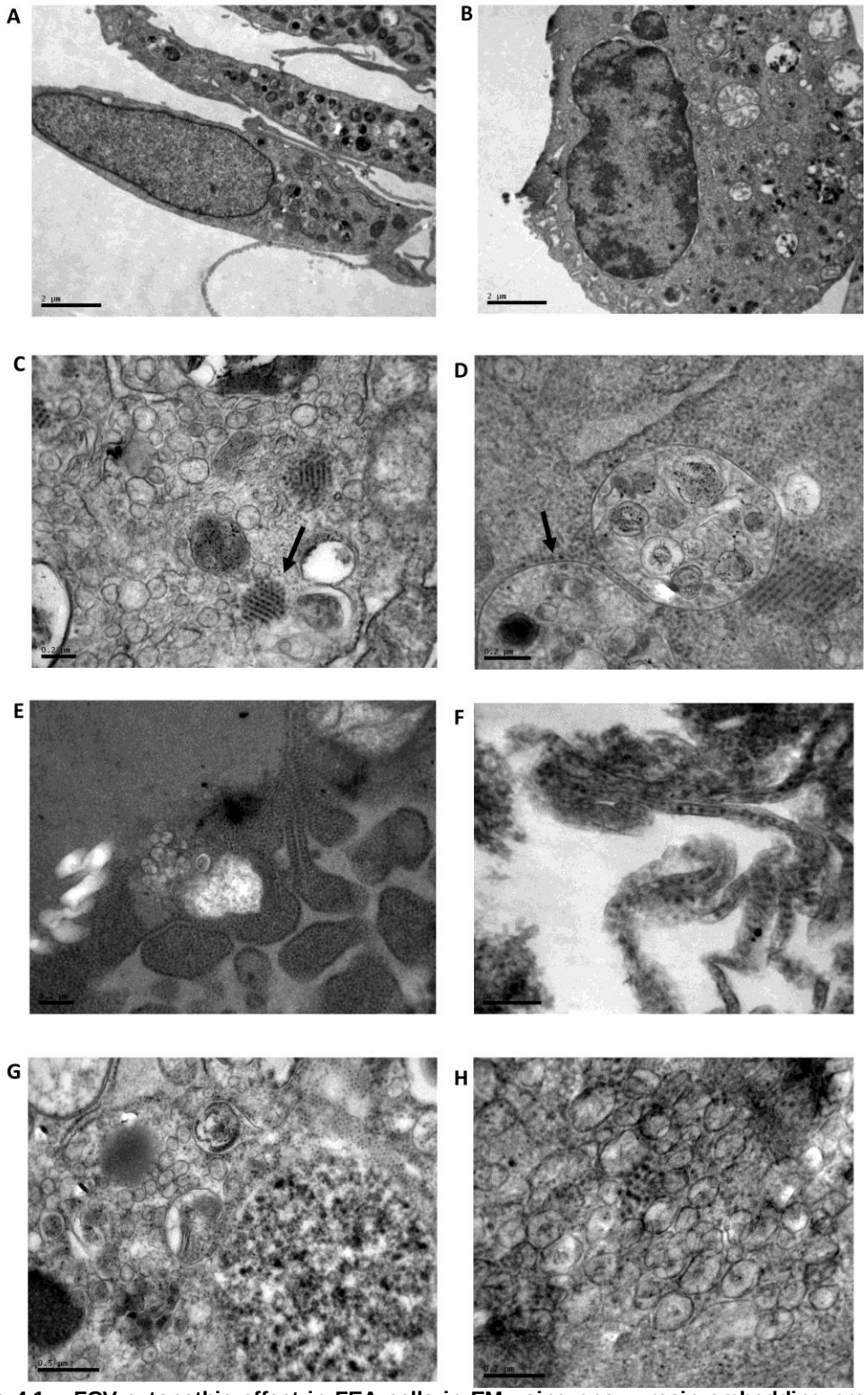

Figure 4.1 – FCV cytopathic effect in FEA cells in EM using epoxy resin embedding preparation. (A) non infected FEA cells, (B) FCV-infected FEA cells 9h post-infection. (C), paracrystaline arrays of FCV particles (arrow). (D) membrane-associated FCV particles (arrow). (E and F) unusual shaped cisternae containing FCV particles. (G and H) FCV-induced membrane-bound vesicles.

Vesicles were frequently located near to a virus cluster, presenting a broad range of sizes with a spherical or elliptical shape (**Fig.4.1G**). These vesicles appeared to have a single membrane bilayer – in contrast to the mitochondria membranes – and to have irregularly shaped dark material generally located at the centre of the vesicle (**Fig.4.1H**). All these features are characteristic of positive-sense RNA viruses as reviewed in the chapter 1.

Golgi apparatus disappearance may be related to the formation of FCV-induced vesicles.

Cytoplasm disorganization was shown to increase over the time of infection. Organelle swallowing was accompanied by an increase in the numbers of vesicles and virus particles per cell. In particular, two organelles showed significant changes throughout the infection: the Golgi apparatus and the ER. In mock-infected cells, the Golgi apparatus was easily observed (**Fig.4.2A**). However, in FCV-infected cells, the Golgi apparatus became more difficult to identify. Still, some cellular structures in early stages of infection resembled the Golgi apparatus. Such an example is the expanded tubular complex associated with smaller vesicles (shown in **Fig.4.2B**). In mock-infected cells, ER was commonly associated with the nucleus but could also be observed far from it. ER in mock-infected cells was present as thin tubular complexes, frequently packed in two or three folds. Although ER was still observed in FCV-infected cells, its morphology was expanded and sometimes it was associated with vesicles that resembled FCV-induced vesicles. It is plausible to admit that since FCV intereferes with the ER, the secretory pathway is also altered, which may lead to the disappearance of the Golgi apparatus.

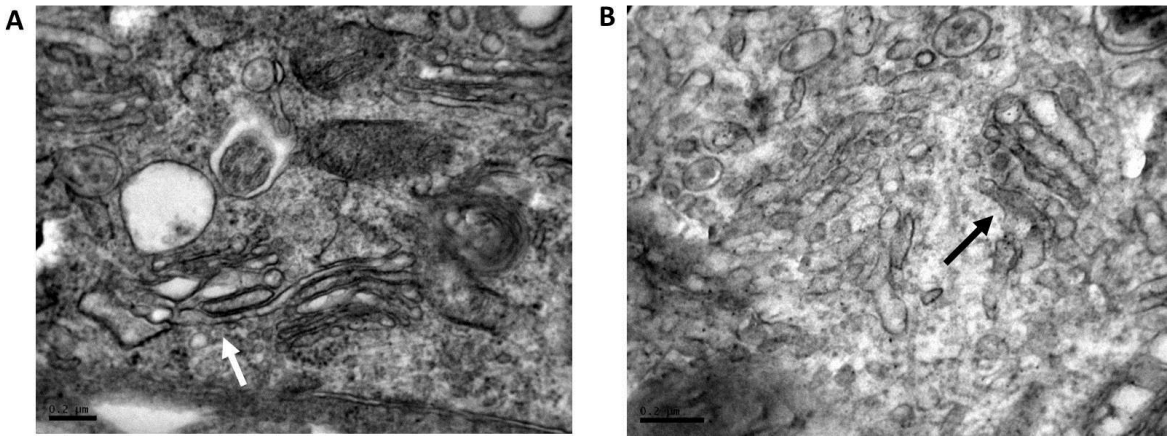

Figure 4.2 - Golgi Apparatus (white arrow) in non-infected cells (A). Unusual tubular shaped compartments (black arrow) in FCV-infected cells 9h post-infection (B).

Tomography and 3D image reconstruction of FCV-infected cells shows that ER is associated with vesicle membranes.

In order to recover three-dimensional information on the spatial organization of FCV-induced vesicles within the cell, a TEM tilt series was performed to generate a tomogram (Suplementary Material 1).

ER expansion and disorganization is closely detailed in **Fig.4.3A**, which shows a frame from the tomogram. Vesicles are found near to compartments that resemble the ER (**Ve** in **Fig.4.3A** and **B**) and in close proximity to arrays of virus particles (**black arrows** in **Fig.4.3**). A closer look at the ER compartment in relation to the vesicles showed that some of the vesicles appear to be membrane-associated (**Fig.4.3C and D**). To further investigate the relationship between ER and vesicles, a three-dimensional image reconstruction of this region was generated as described in Materials and Methods.

The tomographic reconstruction of the ER-vesicles suggests that four vesicles appear to be in contact with the ER compartment (**Fig. 4.3E**). Membranes of the ER and FCV-induced vesicles are represented as a continuous membrane (same density) suggesting that they might be directly associated. These vesicles contain a darker material that was reconstructed as disordered matter (yellow regions in **Fig.4.3E** and **F**). Material of similar density is also found in the lumen of ER with a more random distribution. The ER membrane appears to be thicker than the vesicle membranes, with a rougher surface in contact with the cytoplasm. Some of the vesicle and ER membranes depicted here appear

to have gaps, suggesting a variation of membrane density or even absence in certain regions.

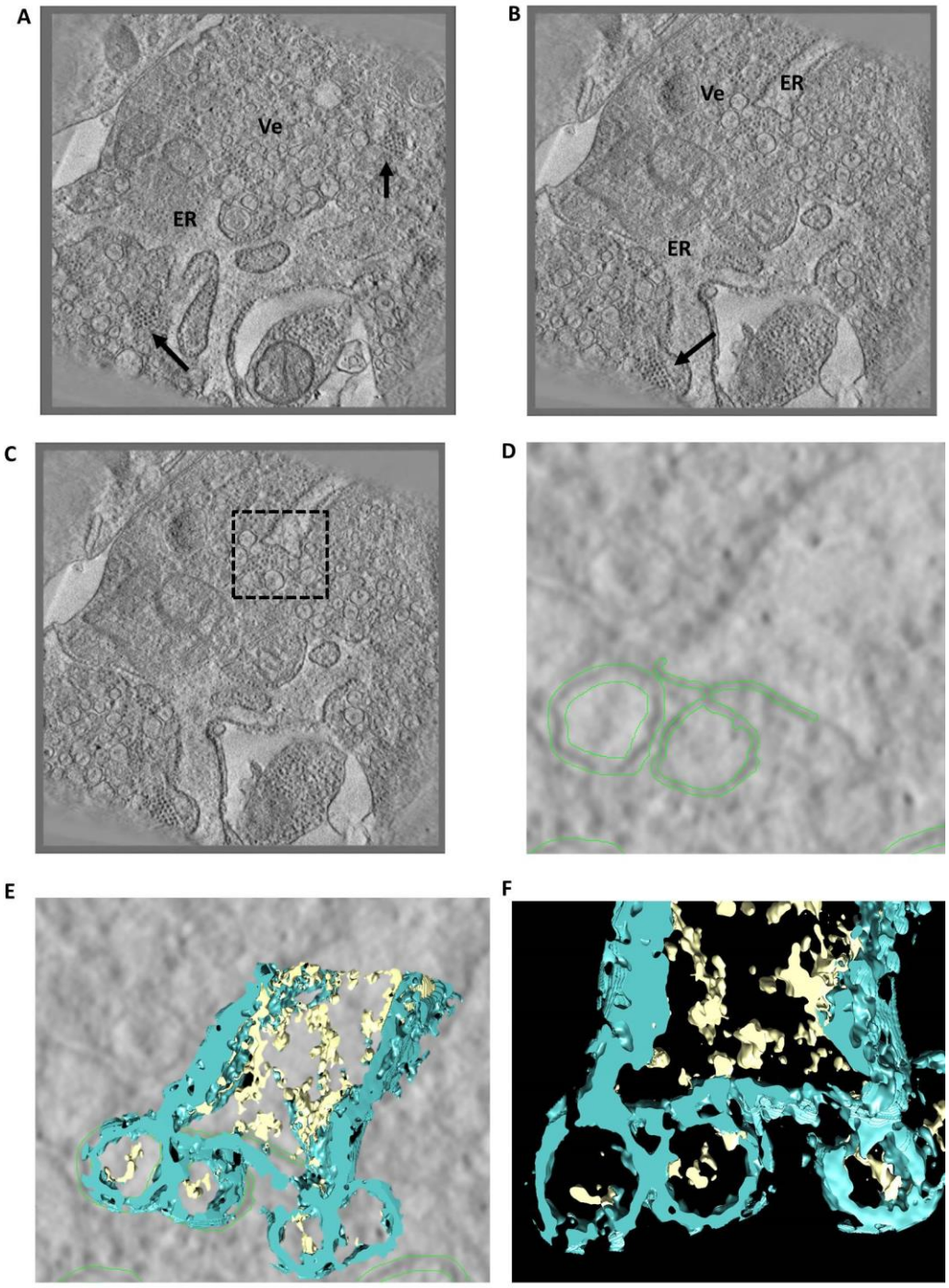

Figure 4.3 – Tomography and 3D image reconstruction of FCV-infected cells shows that ER is associated with vesicle membranes. Slices through a tomogram of a 400nm section of epoxy resin embedded FEA cells infected with FCV (A, B, and C). Ve: FCV-induced membrane-bound vesicles; ER: endoplasmic reticulum; black arrows: FCV

particle arrays. (D) Enlargement of the boxed region in C. (E and F) Three-dimensional reconstruction of FCV induced vesicles in association with ER.

FCV-induced vesicles are organized in a three-dimensional complex with connections between them.

Within the tomogram, a discrete area containing FCV-induced vesicles was isolated and three-dimensional information was retrieved in order to generate an image reconstruction, where vesicles membranes are represented in blue and internal densities in yellow (**Fig.4.4C**). FCV-induced vesicles were distributed across the entire depth of the 400nm section. However, the reconstructed vesicles are depicted as sectioned spheres due to the loss of information at the poles caused by the missing wedge effect (**Fig.4.4D**). Vesicle size varied greatly from 800Å to 2000Å in diameter. No relation was found between the time of infection and the size of vesicles. As previously shown for ER-vesicles reconstructions, vesicles appear to have variations in membrane density and in some cases “holes” are observed in the membrane. The darker material inside the vesicle is not evenly distributed. However, in most cases it is located in the centre with an extended part associated with the membrane (**Fig.4.4C**).

In several cases, vesicles appear to be associated with each other and joined by a small connecting region (**black arrows** in **Fig.4.4B**), the extent of which is better explored in the three-dimensional image reconstruction (**Fig.4.4E**). Overlapping of vesicles appears to occur very often throughout the network; however the contact region is not shown in great detail. A distortion of the membrane was commonly observed at the position of the connection regions between vesicles, resembling a membrane fusion structure (**Fig.4.4F**).

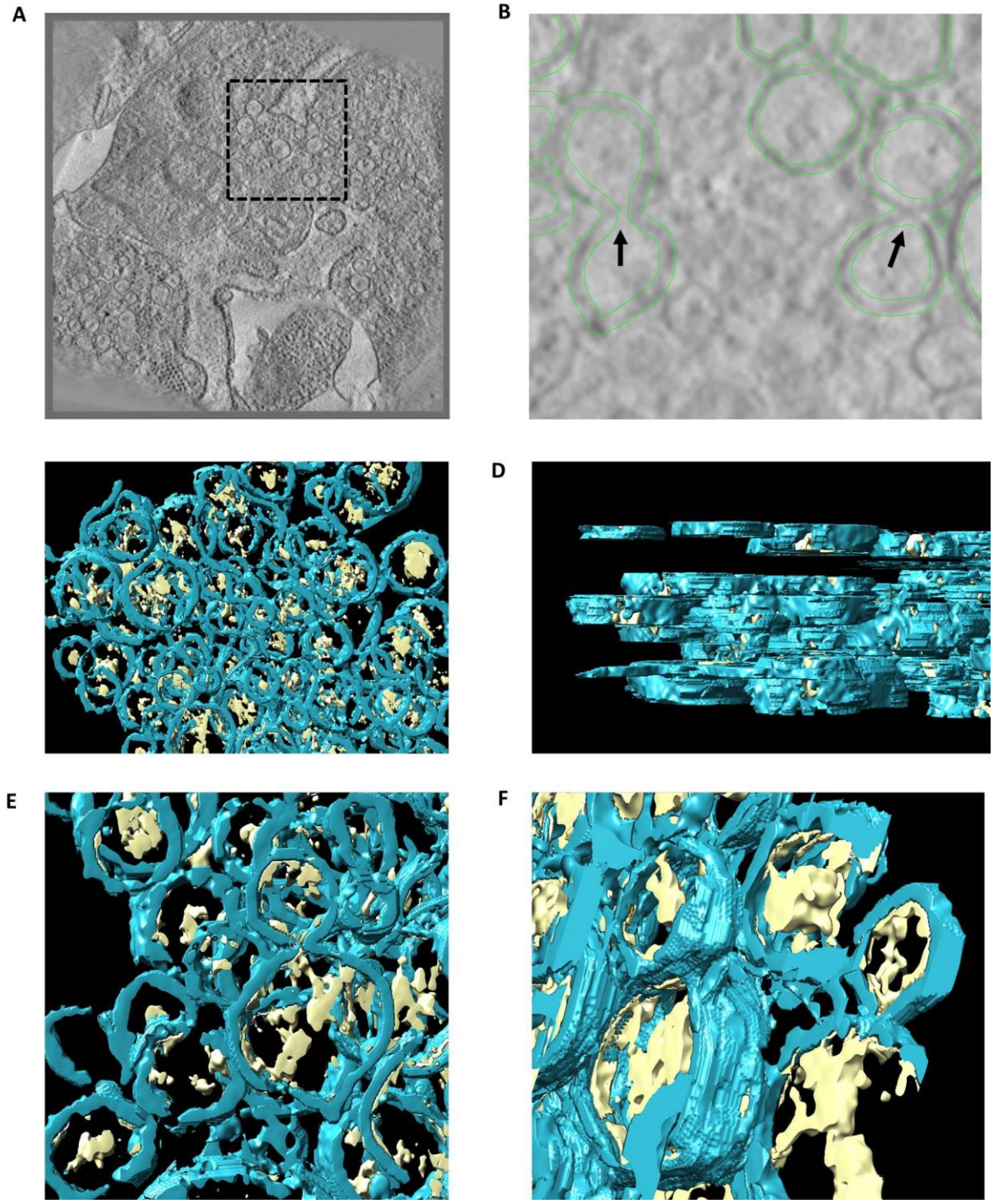

Figure 4.4 – FCV-induced vesicles are organized in a three-dimensional complex with connections between them. Slices through a tomogram of a 400nm section of epoxy resin embedded FEA cells infect with FCV (A), (B) Enlargement of the boxed region in A. (C to E) Three-dimensional reconstruction of FCV induced vesicles in association with ER

4. Discussion

In this study, we analyzed the early stages of FCV infection in FEA cells using electron transmission microscopy. We identified several features characteristic of FCV infection. In all FCV-infected cells observed in this study, vesicles were present in the cytoplasm. As described previously (Love and Sabine 1975, Green, Mory et al. 2002), this is a common feature of caliciviruses and other positive-sense RNA viruses. The number of these vesicles in cells is time-dependent and they often associate with virus particles, suggesting that they have a role in the development of cytopathogenesis.

As shown previously by Green *et al.* (2002), these membranous structures have enzymatic activity and are able to synthesize FCV RNA *in vitro*. A study accomplished by Bailey *et al.* (2010) showed that three non-structural proteins – predicted as transmembrane proteins – are localized to the ER and when co-expressed with a KDEL motif lead to similar membrane rearrangements. Our data suggest that ER and vesicles are directly associated while pronounced rearrangements of ER were observed during infection. Furthermore, the disappearance of the Golgi apparatus in the early stages of infection suggests that FCV may interfere with the vesicular traffic between the ER and the Golgi apparatus.

Some of the FCV-induced vesicles were found to be connected by channels or partially fused. However, the vast majority of vesicles appear to be isolated in the cytoplasm. Also, only vesicles with a considerable diameter (>1300nm) have interconnectivity with other vesicles. Some studies on poliovirus reported similar structures that resemble this connecting regions (Schlegel, Giddings et al. 1996, Egger and Bienz 2002). The apparent connecting regions could be a consequence of the low-resolution of reconstruction of epoxy resin embedding sections. These findings suggest that FCV-induced vesicles may derive primarily from ER, although further in the infection process vesicles can fuse, generating larger compartments for viral RNA replication.

To determine the structural relationship between ER and FCV-induced vesicles, microscopy studies producing greater image detail should be carried out. In alternative to epoxy resin sections, cryo-electron tomography sectioning can be use; in such techniques, sections of the infected cells are performed from the frozen block that maintain the biological structures in its native conformation, providing high-resolution images (Diebolder, Koster et al. 2012).

CONCLUSION

The aim of this work was to elucidate the role of endosomal pH in conformation changes to the capsid and also to understand how FCV-induced replication complexes relate structurally to each other and to organelles in the cell. The main conclusions of our work are:

1. The capsid of FCV undergoes a dramatic conformational change at low pH environment;
2. FCV replication complexes have the ability to associate among themselves and to the ER.

To better assess the extent of the conformational changes observed at low pH, studies that develop an efficient purification procedure for FCV are required. Since, a significant level of purity is necessary for cryoEM and 3D reconstruction, alternative purification methods can also be used. To further explore the mechanism of formation of the FCV-induced vesicles, improved-resolution samples may also be developed. Some alternative methods were suggested, such as cryosectioning, and should be used to explore the structure of FCV-induced vesicles.

We have also compared reconstruction techniques using different software packages in SVLPs. We conclude that:

1. Recombinant SVLPs are structurally similar to other caliciviruses with main differences focused on the organization of P2 domains.
2. Reconstruction techniques can generate different outcomes using the same data. Reconstructions calculated using PTF2/EM3DR showed more consistent features than those calculated using EMAN.

The results herein described contribute to the understanding of FCV biology and infection, in particular, to the interactions between virus and host-cell. The data here reported may also be important to the development of new antiviral drugs and vaccines against VS-FCV.

REFERENCES

Abente, E. J., S. V. Sosnovtsev, C. Sandoval-Jaime, G. I. Parra, K. Bok and K. Y. Green (2013). "The feline calicivirus leader of the capsid protein is associated with cytopathic effect." J Virol **87**(6): 3003-3017.

Abrantes, J., W. van der Loo, J. Le Pendu and P. J. Esteves (2012). "Rabbit haemorrhagic disease (RHD) and rabbit haemorrhagic disease virus (RHDV): a review." Vet Res **43**(1): 12.

Addie, D., H. Poulet, M. C. Golder, M. McDonald, S. Brunet, J. C. Thibault and M. J. Hosie (2008). "Ability of antibodies to two new caliciviral vaccine strains to neutralise feline calicivirus isolates from the UK." Vet Rec **163**(12): 355-357.

Addie, D. D., A. Radford, P. S. Yam and D. J. Taylor (2003). "Cessation of feline calicivirus shedding coincident with resolution of chronic gingivostomatitis in a cat." J Small Anim Pract **44**(4): 172-176.

Adler, J. L. and R. Zickl (1969). "Winter vomiting disease." J Infect Dis **119**(6): 668-673.

Ahlquist, P., A. O. Noueiry, W. M. Lee, D. B. Kushner and B. T. Dye (2003). "Host factors in positive-strand RNA virus genome replication." J Virol **77**(15): 8181-8186.

Auweter, S. D., F. C. Oberstrass and F. H. Allain (2007). "Solving the structure of PTB in complex with pyrimidine tracts: an NMR study of protein-RNA complexes of weak affinities." J Mol Biol **367**(1): 174-186.

Bailey, D., W. J. Kaiser, M. Hollinshead, K. Moffat, Y. Chaudhry, T. Wileman, S. V. Sosnovtsev and I. G. Goodfellow (2010). "Feline calicivirus p32, p39 and p30 proteins localize to the endoplasmic reticulum to initiate replication complex formation." J Gen Virol **91**(Pt 3): 739-749.

Baker, T. S. and R. H. Cheng (1996). "A model-based approach for determining orientations of biological macromolecules imaged by cryoelectron microscopy." J Struct Biol **116**(1): 120-130.

Baltimore, D. (1971). "Expression of animal virus genomes." Bacteriol Rev **35**(3): 235-241.

Bannasch, M. J. and J. E. Foley (2005). "Epidemiologic evaluation of multiple respiratory pathogens in cats in animal shelters." J Feline Med Surg **7**(2): 109-119.

Bartesaghi, A., P. Sprechmann, J. Liu, G. Randall, G. Sapiro and S. Subramaniam (2008). "Classification and 3D averaging with missing wedge correction in biological electron tomography." J Struct Biol **162**(3): 436-450.

Belliot, G., S. V. Sosnovtsev, K. O. Chang, P. McPhie and K. Y. Green (2008). "Nucleotidylylation of the VPg protein of a human norovirus by its proteinase-polymerase precursor protein." Virology **374**(1): 33-49.

Berry, E. S., D. E. Skilling, J. E. Barlough, N. A. Vedros, L. J. Gage and A. W. Smith (1990). "New marine calicivirus serotype infective for swine." Am J Vet Res **51**(8): 1184-1187.

Bhella, D., D. Gatherer, Y. Chaudhry, R. Pink and I. G. Goodfellow (2008). "Structural insights into calicivirus attachment and uncoating." J Virol **82**(16): 8051-8058.

Bhella, D. and I. G. Goodfellow (2011). "The cryo-electron microscopy structure of feline calicivirus bound to junctional adhesion molecule A at 9-angstrom resolution reveals receptor-induced flexibility and two distinct conformational changes in the capsid protein VP1." J Virol **85**(21): 11381-11390.

Bienz, K., D. Egger, M. Troxler and L. Pasamontes (1990). "Structural organization of poliovirus RNA replication is mediated by viral proteins of the P2 genomic region." J Virol **64**(3): 1156-1163.

Binns, S. H., S. Dawson, A. J. Speakman, L. E. Cuevas, C. A. Hart, C. J. Gaskell, K. L. Morgan and R. M. Gaskell (2000). "A study of feline upper respiratory tract disease with reference to

prevalence and risk factors for infection with feline calicivirus and feline herpesvirus." J Feline Med Surg **2**(3): 123-133.

Bittle, J. L. and W. J. Rubic (1976). "Immunization against feline calicivirus infection." Am J Vet Res **37**(3): 275-278.

Bostina, M., H. Levy, D. J. Filman and J. M. Hogle (2011). "Poliovirus RNA is released from the capsid near a twofold symmetry axis." J Virol **85**(2): 776-783.

Bridger, J. C., G. A. Hall and J. F. Brown (1984). "Characterization of a calici-like virus (Newbury agent) found in association with astrovirus in bovine diarrhea." Infect Immun **43**(1): 133-138.

Burki, F. (1965). "Picornaviruses of cats." Arch Gesamte Virusforsch **15**(5): 690-696.

Burroughs, J. N. and F. Brown (1978). "Presence of a covalently linked protein on calicivirus RNA." J Gen Virol **41**(2): 443-446.

Cancio-Lonches, C., M. Yocupicio-Monroy, C. Sandoval-Jaime, I. Galvan-Mendoza, L. Urena, S. Vashist, I. Goodfellow, J. Salas-Benito and A. L. Gutierrez-Escolano (2011). "Nucleolin interacts with the feline calicivirus 3' untranslated region and the protease-polymerase NS6 and NS7 proteins, playing a role in virus replication." J Virol **85**(16): 8056-8068.

Carter, M. J. (1989). "Feline calicivirus protein synthesis investigated by western blotting." Arch Virol **108**(1-2): 69-79.

Carter, M. J., I. D. Milton, J. Meanger, M. Bennett, R. M. Gaskell and P. C. Turner (1992). "The complete nucleotide sequence of a feline calicivirus." Virology **190**(1): 443-448.

Chang, K.-O., Y. Kim, K. Y. Green and L. J. Saif (2002). "Cell-Culture Propagation of Porcine Enteric Calicivirus Mediated by Intestinal Contents Is Dependent on the Cyclic AMP Signaling Pathway." Virology **304**(2): 302-310.

Chang, K. O., D. W. George, J. B. Patton, K. Y. Green and S. V. Sosnovtsev (2008). "Leader of the capsid protein in feline calicivirus promotes replication of Norwalk virus in cell culture." J Virol **82**(19): 9306-9317.

Chaudhry, Y., A. Nayak, M. E. Bordeleau, J. Tanaka, J. Pelletier, G. J. Belsham, L. O. Roberts and I. G. Goodfellow (2006). "Caliciviruses differ in their functional requirements for eIF4F components." J Biol Chem **281**(35): 25315-25325.

Chen, R., J. D. Neill, M. K. Estes and B. V. Prasad (2006). "X-ray structure of a native calicivirus: structural insights into antigenic diversity and host specificity." Proc Natl Acad Sci U S A **103**(21): 8048-8053.

Chen, Y., C. P. Liang, Y. Liu, A. H. Fischer, A. V. Parwani and L. Pantanowitz (2012). "Review of advanced imaging techniques." J Pathol Inform **3**: 22.

Chiba, S., S. Nakata, K. Numata-Kinoshita and S. Honma (2000). "Sapporo virus: history and recent findings." J Infect Dis **181 Suppl 2**: S303-308.

Chiba, S., Y. Sakuma, R. Kogasaka, M. Akihara, K. Horino, T. Nakao and S. Fukui (1979). "An outbreak of gastroenteritis associated with calicivirus in an infant home." J Med Virol **4**(4): 249-254.

Clarke, I. N. and P. R. Lambden (1997). "The molecular biology of caliciviruses." J Gen Virol **78 (Pt 2)**: 291-301.

Clay, S., S. Maherchandani, Y. S. Malik and S. M. Goyal (2006). "Survival on uncommon fomites of feline calicivirus, a surrogate of noroviruses." Am J Infect Control **34**(1): 41-43.

Cohen, J. (2013). "Structural biology. Is high-tech view of HIV too good to be true?" Science **341**(6145): 443-444.

Coyne, K. P., R. M. Christley, O. G. Pybus, S. Dawson, R. M. Gaskell and A. D. Radford (2012). "Large-scale spatial and temporal genetic diversity of feline calicivirus." J Virol **86**(20): 11356-11367.

Coyne, K. P., S. Dawson, A. D. Radford, P. J. Cripps, C. J. Porter, C. M. McCracken and R. M. Gaskell (2006). "Long-term analysis of feline calicivirus prevalence and viral shedding patterns in naturally infected colonies of domestic cats." Vet Microbiol **118**(1–2): 12-25.

Coyne, K. P., R. M. Gaskell, S. Dawson, C. J. Porter and A. D. Radford (2007). "Evolutionary mechanisms of persistence and diversification of a calicivirus within endemically infected natural host populations." J Virol **81**(4): 1961-1971.

Coyne, K. P., F. C. Reed, C. J. Porter, S. Dawson, R. M. Gaskell and A. D. Radford (2006). "Recombination of Feline calicivirus within an endemically infected cat colony." J Gen Virol **87**(Pt 4): 921-926.

Danthi, P., K. M. Guglielmi, E. Kirchner, B. Mainou, T. Stehle and T. S. Dermody (2010). "From touchdown to transcription: the reovirus cell entry pathway." Curr Top Microbiol Immunol **343**: 91-119.

Danthi, P., M. Tosteson, Q. H. Li and M. Chow (2003). "Genome delivery and ion channel properties are altered in VP4 mutants of poliovirus." J Virol **77**(9): 5266-5274.

Datta, U. and A. Dasgupta (1994). "Expression and subcellular localization of poliovirus VPg-precursor protein 3AB in eukaryotic cells: evidence for glycosylation in vitro." J Virol **68**(7): 4468-4477.

den Boon, J. A. and P. Ahlquist (2010). "Organelle-like membrane compartmentalization of positive-strand RNA virus replication factories." Annu Rev Microbiol **64**: 241-256.

Di Bartolo, I., E. Ponterio, M. Monini and F. M. Ruggeri (2011). "A pilot survey of bovine norovirus in northern Italy." Vet Rec **169**(3): 73.

Di Martino, B., C. Di Rocco, C. Ceci and F. Marsilio (2009). "Characterization of a strain of feline calicivirus isolated from a dog faecal sample." Vet Microbiol **139**(1-2): 52-57.

Di Martino, B. and F. Marsilio (2010). "Feline calicivirus VP2 is involved in the self-assembly of the capsid protein into virus-like particles." Res Vet Sci **89**(2): 279-281.

Di Martino, B., F. Marsilio and P. Roy (2007). "Assembly of feline calicivirus-like particle and its immunogenicity." Vet Microbiol **120**(1-2): 173-178.

Diebolder, C. A., A. J. Koster and R. I. Koning (2012). "Pushing the resolution limits in cryo electron tomography of biological structures." J Microsc **248**(1): 1-5.

Dobro, M. J., L. A. Melanson, G. J. Jensen and A. W. McDowall (2010). "Plunge freezing for electron cryomicroscopy." Methods Enzymol **481**: 63-82.

Domingo, E., L. Menendez-Arias and J. J. Holland (1997). "RNA virus fitness." Rev Med Virol **7**(2): 87-96.

Doultree, J. C., J. D. Druce, C. J. Birch, D. S. Bowden and J. A. Marshall (1999). "Inactivation of feline calicivirus, a Norwalk virus surrogate." J Hosp Infect **41**(1): 51-57.

Drake, J. W. (1993). "Rates of spontaneous mutation among RNA viruses." Proc Natl Acad Sci U S A **90**(9): 4171-4175.

Egger, D. and K. Bienz (2002). "Recombination of poliovirus RNA proceeds in mixed replication complexes originating from distinct replication start sites." J Virol **76**(21): 10960-10971.

Egger, D., N. Teterina, E. Ehrenfeld and K. Bienz (2000). "Formation of the poliovirus replication complex requires coupled viral translation, vesicle production, and viral RNA synthesis." J Virol **74**(14): 6570-6580.

Elena, S. F. and R. Sanjuan (2005). "Adaptive value of high mutation rates of RNA viruses: separating causes from consequences." J Virol **79**(18): 11555-11558.

Etherington, G. J., S. M. Ring, M. A. Charleston, J. Dicks, V. J. Rayward-Smith and I. N. Roberts (2006). "Tracing the origin and co-phylogeny of the caliciviruses." J Gen Virol **87**(5): 1229-1235.

Fastier, L. B. (1957). "A new feline virus isolated in tissue culture." Am J Vet Res **18**(67): 382-389.

Fenner, F. (1976). "The classification and nomenclature of viruses. Summary of results of meetings of the International Committee on Taxonomy of Viruses in Madrid, September 1975." Virology **71**(2): 371-378.

Fernández, J. J., D. Luque, J. R. Castón and J. L. Carrascosa (2008). "Sharpening high resolution information in single particle electron cryomicroscopy." J Struct Biol **164**(1): 170-175.

Fretz, M. and F. L. Schaffer (1978). "Calicivirus proteins in infected cells: evidence for a capsid polypeptide precursor." Virology **89**(1): 318-321.

Fricks, C. E. and J. M. Hogle (1990). "Cell-induced conformational change in poliovirus: externalization of the amino terminus of VP1 is responsible for liposome binding." J Virol **64**(5): 1934-1945.

Gagescu, R., N. Demaurex, R. G. Parton, W. Hunziker, L. A. Huber and J. Gruenberg (2000). "The recycling endosome of Madin-Darby canine kidney cells is a mildly acidic compartment rich in raft components." Mol Biol Cell **11**(8): 2775-2791.

Gaskell, C. J., R. M. Gaskell, P. E. Dennis and M. J. Wooldridge (1982). "Efficacy of an inactivated feline calicivirus (FCV) vaccine against challenge with United Kingdom field strains and its interaction with the FCV carrier state." Res Vet Sci **32**(1): 23-26.

Geissler, K., K. Schneider and U. Truyen (2002). "Mapping neutralizing and non-neutralizing epitopes on the capsid protein of feline calicivirus." J Vet Med B Infect Dis Vet Public Health **49**(1): 55-60.

Gerke, V. and S. E. Moss (2002). "Annexins: from structure to function." Physiol Rev **82**(2): 331-371.

Gingras, A. C., B. Raught and N. Sonenberg (1999). "eIF4 initiation factors: effectors of mRNA recruitment to ribosomes and regulators of translation." Annu Rev Biochem **68**: 913-963.

Glaeser, R. M. (2008). "Retrospective: radiation damage and its associated "information limitations"." J Struct Biol **163**(3): 271-276.

Glenn, M., A. D. Radford, P. C. Turner, M. Carter, D. Lowery, D. A. DeSilver, J. Meanger, C. Baulch-Brown, M. Bennett and R. M. Gaskell (1999). "Nucleotide sequence of UK and Australian isolates of feline calicivirus (FCV) and phylogenetic analysis of FCVs." Vet Microbiol **67**(3): 175-193.

Goodfellow, I., Y. Chaudhry, I. Gioldasi, A. Gerondopoulos, A. Natoni, L. Labrie, J. F. Laliberte and L. Roberts (2005). "Calicivirus translation initiation requires an interaction between VPg and eIF 4 E." EMBO Rep **6**(10): 968-972.

Gore, T. C., N. Lakshmanan, J. R. Williams, F. F. Jirjis, S. T. Chester, K. L. Duncan, M. J. Coyne, M. A. Lum and F. J. Sterner (2006). "Three-year duration of immunity in cats following vaccination against feline rhinotracheitis virus, feline calicivirus, and feline panleukopenia virus." Vet Ther **7**(3): 213-222.

Green, K. Y., A. Mory, M. H. Fogg, A. Weisberg, G. Belliot, M. Wagner, T. Mitra, E. Ehrenfeld, C. E. Cameron and S. V. Sosnovtsev (2002). "Isolation of enzymatically active replication complexes from feline calicivirus-infected cells." J Virol **76**(17): 8582-8595.

Grishaev, A. (2012). Sample preparation, data collection, and preliminary data analysis in biomolecular solution X-ray scattering.

Guix, S., M. Asanaka, K. Katayama, S. E. Crawford, F. H. Neill, R. L. Atmar and M. K. Estes (2007). "Norwalk virus RNA is infectious in mammalian cells." J Virol **81**(22): 12238-12248.

Hansman, G. S., S. Ishida, S. Yoshizumi, M. Miyoshi, T. Ikeda, T. Oka and N. Takeda (2007). "Recombinant sapovirus gastroenteritis, Japan." Emerg Infect Dis **13**(5): 786-788.

Hansman, G. S., K. Katayama, N. Maneekarn, S. Peerakome, P. Khamrin, S. Tonusin, S. Okitsu, O. Nishio, N. Takeda and H. Ushijima (2004). "Genetic diversity of norovirus and sapovirus in hospitalized infants with sporadic cases of acute gastroenteritis in Chiang Mai, Thailand." J Clin Microbiol **42**(3): 1305-1307.

Hansman, G. S., K. Natori, T. Oka, S. Ogawa, K. Tanaka, N. Nagata, H. Ushijima, N. Takeda and K. Katayama (2005). "Cross-reactivity among sapovirus recombinant capsid proteins." Arch Virol **150**(1): 21-36.

Hansman, G. S., T. Oka and N. Takeda (2008). "Sapovirus-like particles derived from polyprotein." Virus Research **137**(2): 261-265.

Harbour, D. A., P. E. Howard and R. M. Gaskell (1991). "Isolation of feline calicivirus and feline herpesvirus from domestic cats 1980 to 1989." Vet Rec **128**(4): 77-80.

Hashimoto, M., F. Roerink, Y. Tohya and M. Mochizuki (1999). "Genetic analysis of the RNA polymerase gene of caliciviruses from dogs and cats." J Vet Med Sci **61**(6): 603-608.

Henderson, R. and G. McMullan (2013). "Problems in obtaining perfect images by single-particle electron cryomicroscopy of biological structures in amorphous ice." Microscopy (Oxf) **62**(1): 43-50.

Herbert, T. P., I. Brierley and T. D. Brown (1997). "Identification of a protein linked to the genomic and subgenomic mRNAs of feline calicivirus and its role in translation." J Gen Virol **78 (Pt 5)**: 1033-1040.

Heymann, J. B. (2001). "Bsoft: image and molecular processing in electron microscopy." J Struct Biol **133**(2-3): 156-169.

Hoover, E. A. and D. E. Kahn (1975). "Experimentally induced feline calicivirus infection: clinical signs and lesions." J Am Vet Med Assoc **166**(5): 463-468.

Hopkins, S. R. (1958). "The growth and cytopathogenicity of vesicular exanthema virus in swine kidney tissue culture." Am J Vet Res **19**(71): 497-499.

Huang, C., J. Hess, M. Gill and D. Hustead (2010). "A dual-strain feline calicivirus vaccine stimulates broader cross-neutralization antibodies than a single-strain vaccine and lessens clinical signs in vaccinated cats when challenged with a homologous feline calicivirus strain associated with virulent systemic disease." J Feline Med Surg **12**(2): 129-137.

Hurley, K. E., P. A. Pesavento, N. C. Pedersen, A. M. Poland, E. Wilson and J. E. Foley (2004). "An outbreak of virulent systemic feline calicivirus disease." J Am Vet Med Assoc **224**(2): 241-249.

ICTV, A. M. Q. King, E. Lefkowitz, M. J. Adams and E. B. Carstens (2012). "Virus Taxonomy: Ninth Report of the International Committee on Taxonomy of Viruses."

Jackson, W. T., T. H. Giddings, Jr., M. P. Taylor, S. Mulinyawe, M. Rabinovitch, R. R. Kopito and K. Kirkegaard (2005). "Subversion of cellular autophagosomal machinery by RNA viruses." PLoS Biol **3**(5): e156.

Jensen, G. (2010). "Cryo-EM, Part A: sample preparation and data collection. Preface." Methods Enzymol **481**: xv-xvi.

Kaiser, W. J., Y. Chaudhry, S. V. Sosnovtsev and I. G. Goodfellow (2006). "Analysis of protein-protein interactions in the feline calicivirus replication complex." J Gen Virol **87**(Pt 2): 363-368.

Karakasiliotis, I., Y. Chaudhry, L. O. Roberts and I. G. Goodfellow (2006). "Feline calicivirus replication: requirement for polypyrimidine tract-binding protein is temperature-dependent." J Gen Virol **87**(Pt 11): 3339-3347.

Karakasiliotis, I., S. Vashist, D. Bailey, E. J. Abente, K. Y. Green, L. O. Roberts, S. V. Sosnovtsev and I. G. Goodfellow (2010). "Polypyrimidine tract binding protein functions as a negative regulator of feline calicivirus translation." PLoS One **5**(3): e9562.

Katayama, K., T. Miyoshi, K. Uchino, T. Oka, T. Tanaka, N. Takeda and G. S. Hansman (2004). "Novel recombinant sapovirus." Emerg Infect Dis **10**(10): 1874-1876.

Kausche, G., E. Pfankuch and H. Ruska (1939). "Die Sichtbarmachung von pflanzlichem Virus im Ubermikroskop." Naturwissenschaften **27**: 8.

Khan, K. N., G. J. Kociba, M. L. Wellman and J. A. Reiter (1992). "Cytotoxicity in feline leukemia virus subgroup-C infected fibroblasts is mediated by adherent bone marrow mononuclear cells." In Vitro Cell Dev Biol **28A**(4): 260-266.

Kostrewa, D., M. Brockhaus, A. D'Arcy, G. E. Dale, P. Nelboeck, G. Schmid, F. Mueller, G. Bazzoni, E. Dejana, T. Bartfai, F. K. Winkler and M. Hennig (2001). "X-ray structure of junctional adhesion molecule: structural basis for homophilic adhesion via a novel dimerization motif." EMBO J **20**(16): 4391-4398.

Kreutz, L. C., R. P. Johnson and B. S. Seal (1998). "Phenotypic and genotypic variation of feline calicivirus during persistent infection of cats." Vet Microbiol **59**(2-3): 229-236.

Kreutz, L. C. and B. S. Seal (1995). "The pathway of feline calicivirus entry." Virus Res **35**(1): 63-70.

Kreutz, L. C., B. S. Seal and W. L. Mengeling (1994). "Early interaction of feline calicivirus with cells in culture." Arch Virol **136**(1-2): 19-34.

L'Homme, Y., J. Brassard, M. Ouardani and M. J. Gagne (2010). "Characterization of novel porcine sapoviruses." Arch Virol **155**(6): 839-846.

Lama, J., A. V. Paul, K. S. Harris and E. Wimmer (1994). "Properties of purified recombinant poliovirus protein 3aB as substrate for viral proteinases and as co-factor for RNA polymerase 3Dpol." J Biol Chem **269**(1): 66-70.

Leen, E. N., K. Y. Kwok, J. R. Birtley, P. J. Simpson, C. V. Subba-Reddy, Y. Chaudhry, S. V. Sosnovtsev, K. Y. Green, S. N. Prater, M. Tong, J. C. Young, L. M. Chung, J. Marchant, L. O. Roberts, C. C. Kao, S. Matthews, I. G. Goodfellow and S. Curry (2013). "Structures of the compact helical core domains of feline calicivirus and murine norovirus VPg proteins." J Virol **87**(10): 5318-5330.

Lesbros, C., V. Martin, W. Najbar, A. Sanquer, D. McGahie, H. M. Eun and S. Gueguen (2013). "Protective Efficacy of the Calicivirus Valency of the Leucofeligen Vaccine against a Virulent Heterologous Challenge in Kittens." Vet Med Int **2013**: 232397.

Leung, W. K., P. K. Chan, N. L. Lee and J. J. Sung (2010). "Development of an in vitro cell culture model for human noroviruses and its clinical application." Hong Kong Med J **16**(5 Suppl 4): 18-21.

Liu, S. H., M. L. Wong, C. S. Craik and F. M. Brodsky (1995). "Regulation of clathrin assembly and trimerization defined using recombinant triskelion hubs." Cell **83**(2): 257-267.

Love, D. N. and M. Sabine (1975). "Electron microscopic observation of feline kidney cells infected with a feline calicivirus." Arch Virol **48**(3): 213-228.

Makino, A., M. Shimojima, T. Miyazawa, K. Kato, Y. Tohya and H. Akashi (2006). "Junctional adhesion molecule 1 is a functional receptor for feline calicivirus." J Virol **80**(9): 4482-4490.

Mao, Y., L. Wang, C. Gu, A. Herschhorn, A. Désormeaux, A. Finzi, S.-H. Xiang and J. G. Sodroski (2013). "Molecular architecture of the uncleaved HIV-1 envelope glycoprotein trimer." Proc Natl Acad Sci U S A.

Marsilio, F., B. Di Martino, N. Decaro and C. Buonavoglia (2005). "A novel nested PCR for the diagnosis of calicivirus infections in the cat." Vet Microbiol **105**(1): 1-7.

Martella, V., E. Lorusso, N. Decaro, G. Elia, A. Radogna, M. D'Abramo, C. Desario, A. Cavalli, M. Corrente, M. Camero, C. A. Germinario, K. Banyai, B. Di Martino, F. Marsilio, L. E. Carmichael and C. Buonavoglia (2008). "Detection and molecular characterization of a canine norovirus." Emerg Infect Dis **14**(8): 1306-1308.

Martella, V., A. Pratelli, M. Gentile, D. Buonavoglia, N. Decaro, P. Fiorente and C. Buonavoglia (2002). "Analysis of the capsid protein gene of a feline-like calicivirus isolated from a dog." Vet Microbiol **85**(4): 315-322.

Martin-Padura, I., S. Lostaglio, M. Schneemann, L. Williams, M. Romano, P. Fruscella, C. Panzeri, A. Stoppacciaro, L. Ruco, A. Villa, D. Simmons and E. Dejana (1998). "Junctional adhesion

molecule, a novel member of the immunoglobulin superfamily that distributes at intercellular junctions and modulates monocyte transmigration." J Cell Biol **142**(1): 117-127.

Masubuchi, K., A. Wakatsuki, K. Iwamoto, T. Takahashi, T. Kokubu and M. Shimizu (2010). "Immunological and genetic characterization of feline caliciviruses used in the development of a new trivalent inactivated vaccine in Japan." J Vet Med Sci **72**(9): 1189-1194.

Matsuura, Y., Y. Tohya, M. Mochizuki, K. Takase and T. Sugimura (2001). "Identification of conformational neutralizing epitopes on the capsid protein of canine calicivirus." J Gen Virol **82**(Pt 7): 1695-1702.

Mattison, K., A. Shukla, A. Cook, F. Pollari, R. Friendship, D. Kelton, S. Bidawid and J. M. Farber (2007). "Human noroviruses in swine and cattle." Emerg Infect Dis **13**(8): 1184-1188.

Mencke, N., M. Vobis, H. Mehlhorn, D. H. J, M. Rehagen, S. Mangold-Gehring and U. Truyen (2009). "Transmission of feline calicivirus via the cat flea (Ctenocephalides felis)." Parasitol Res **105**(1): 185-189.

Mitchell, S. A., K. A. Spriggs, M. J. Coldwell, R. J. Jackson and A. E. Willis (2003). "The Apaf-1 internal ribosome entry segment attains the correct structural conformation for function via interactions with PTB and unr." Mol Cell **11**(3): 757-771.

Mochizuki, M., A. Kawanishi, H. Sakamoto, S. Tashiro, R. Fujimoto and M. Ohwaki (1993). "A calicivirus isolated from a dog with fatal diarrhoea." Vet Rec **132**(9): 221-222.

Mousavi, S. A., L. Malerod, T. Berg and R. Kjeken (2004). "Clathrin-dependent endocytosis." Biochem J **377**(Pt 1): 1-16.

Moya, A., E. C. Holmes and F. Gonzalez-Candelas (2004). "The population genetics and evolutionary epidemiology of RNA viruses." Nat Rev Microbiol **2**(4): 279-288.

Natoni, A., G. E. Kass, M. J. Carter and L. O. Roberts (2006). "The mitochondrial pathway of apoptosis is triggered during feline calicivirus infection." J Gen Virol **87**(Pt 2): 357-361.

Neill, J. D. (1992). "Nucleotide sequence of the capsid protein gene of two serotypes of San Miguel sea lion virus: identification of conserved and non-conserved amino acid sequences among calicivirus capsid proteins." Virus Res **24**(2): 211-222.

Neill, J. D. and W. L. Mengeling (1988). "Further characterization of the virus-specific RNAs in feline calicivirus infected cells." Virus Research **11**(1): 59-72.

Neill, J. D., I. M. Reardon and R. L. Heinrikson (1991). "Nucleotide sequence and expression of the capsid protein gene of feline calicivirus." J Virol **65**(10): 5440-5447.

Ng, K. K., M. M. Cherney, A. L. Vazquez, A. Machin, J. M. Alonso, F. Parra and M. N. James (2002). "Crystal structures of active and inactive conformations of a caliciviral RNA-dependent RNA polymerase." J Biol Chem **277**(2): 1381-1387.

Nilsson, M., K. O. Hedlund, M. Thorhagen, G. Larson, K. Johansen, A. Ekspong and L. Svensson (2003). "Evolution of human calicivirus RNA in vivo: accumulation of mutations in the protruding P2 domain of the capsid leads to structural changes and possibly a new phenotype." J Virol **77**(24): 13117-13124.

O'Reilly, A. M. W. K. J. (1969). "The development of feline cell lines for the growth of feline infectious enteritis (panleucopaenia) virus." Journal of Hygiene **67**(1): 10.

O'Reilly, E. K. and C. C. Kao (1998). "Analysis of RNA-dependent RNA polymerase structure and function as guided by known polymerase structures and computer predictions of secondary structure." Virology **252**(2): 287-303.

Ohe, K., T. Takahashi, D. Hara and M. Hara (2008). "Sensitivity of FCV to recombinant feline interferon (rFeIFN)." Vet Res Commun **32**(2): 167-174.

Ohlinger, V. F., B. Haas, G. Meyers, F. Weiland and H. J. Thiel (1990). "Identification and characterization of the virus causing rabbit hemorrhagic disease." J Virol **64**(7): 3331-3336.

Orlova, E. V. and H. R. Saibil (2011). "Structural analysis of macromolecular assemblies by electron microscopy." Chem Rev **111**(12): 7710-7748.

Ossiboff, R. J. and J. S. Parker (2007). "Identification of regions and residues in feline junctional adhesion molecule required for feline calicivirus binding and infection." J Virol **81**(24): 13608-13621.

Ossiboff, R. J., Y. Zhou, P. J. Lightfoot, B. V. Prasad and J. S. Parker (2010). "Conformational changes in the capsid of a calicivirus upon interaction with its functional receptor." J Virol **84**(11): 5550-5564.

Pang, X. L., B. E. Lee, G. J. Tyrrell and J. K. Preiksaitis (2009). "Epidemiology and genotype analysis of sapovirus associated with gastroenteritis outbreaks in Alberta, Canada: 2004-2007." J Infect Dis **199**(4): 547-551.

Patel, M. M., A. J. Hall, J. Vinje and U. D. Parashar (2009). "Noroviruses: a comprehensive review." J Clin Virol **44**(1): 1-8.

Patel, M. M., M. A. Widdowson, R. I. Glass, K. Akazawa, J. Vinje and U. D. Parashar (2008). "Systematic literature review of role of noroviruses in sporadic gastroenteritis." Emerg Infect Dis **14**(8): 1224-1231.

Paul, A. V., A. Schultz, S. E. Pincus, S. Oroszlan and E. Wimmer (1987). "Capsid protein VP4 of poliovirus is N-myristoylated." Proc Natl Acad Sci U S A **84**(22): 7827-7831.

Pearse, B. M., C. J. Smith and D. J. Owen (2000). "Clathrin coat construction in endocytosis." Curr Opin Struct Biol **10**(2): 220-228.

Pedersen, N. C., J. B. Elliott, A. Glasgow, A. Poland and K. Keel (2000). "An isolated epizootic of hemorrhagic-like fever in cats caused by a novel and highly virulent strain of feline calicivirus." Veterinary Microbiology **73**(4): 281-300.

Pesavento, P. A., K.-O. Chang and J. S. L. Parker (2008). "Molecular Virology of Feline Calicivirus." Veterinary Clinics of North America: Small Animal Practice **38**(4): 775-786.

Pesavento, P. A., K. O. Chang and J. S. Parker (2008). "Molecular virology of feline calicivirus." Vet Clin North Am Small Anim Pract **38**(4): 775-786, vii.

Pesavento, P. A., N. J. MacLachlan, L. Dillard-Telm, C. K. Grant and K. F. Hurley (2004). "Pathologic, Immunohistochemical, and Electron Microscopic Findings in Naturally Occurring Virulent Systemic Feline Calicivirus Infection in Cats." Vet Pathol **41**: 8.

Pesavento, P. A., T. Stokol, H. Liu, D. A. van der List, P. M. Gaffney and J. S. Parker (2011). "Distribution of the feline calicivirus receptor junctional adhesion molecule a in feline tissues." Vet Pathol **48**(2): 361-368.

Pettersen, E. F., T. D. Goddard, C. C. Huang, G. S. Couch, D. M. Greenblatt, E. C. Meng and T. E. Ferrin (2004). "UCSF Chimera--a visualization system for exploratory research and analysis." J Comput Chem **25**(13): 1605-1612.

Porter, C. J., A. D. Radford, R. M. Gaskell, R. Ryvar, K. P. Coyne, G. L. Pinchbeck and S. Dawson (2008). "Comparison of the ability of feline calicivirus (FCV) vaccines to neutralise a panel of current UK FCV isolates." J Feline Med Surg **10**(1): 32-40.

Poulet, H., S. Brunet, V. Leroy and G. Chappuis (2005). "Immunisation with a combination of two complementary feline calicivirus strains induces a broad cross-protection against heterologous challenges." Vet Microbiol **106**(1-2): 17-31.

Povey, C. and J. Ingersoll (1975). "Cross-protection among feline caliciviruses." Infect Immun **11**(5): 877-885.

Povey, R. C. (1978). "Effect of orally administered ribavirin on experimental feline calicivirus infection in cats." Am J Vet Res **39**(8): 1337-1341.

Povey, R. C., H. Koonse and M. B. Hays (1980). "Immunogenicity and safety of an inactivated vaccine for the prevention of rhinotracheitis, caliciviral disease, and panleukopenia in cats." J Am Vet Med Assoc **177**(4): 347-350.

Prasad, B. V., M. E. Hardy, T. Dokland, J. Bella, M. G. Rossmann and M. K. Estes (1999). "X-ray crystallographic structure of the Norwalk virus capsid." Science **286**(5438): 287-290.

Prasad, B. V., D. O. Matson and A. W. Smith (1994). "Three-dimensional structure of calicivirus." J Mol Biol **240**(3): 256-264.

Radford, A. D., D. Addie, S. Belak, C. Boucraut-Baralon, H. Egberink, T. Frymus, T. Gruffydd-Jones, K. Hartmann, M. J. Hosie, A. Lloret, H. Lutz, F. Marsilio, M. G. Pennisi, E. Thiry, U. Truyen and M. C. Horzinek (2009). "Feline calicivirus infection. ABCD guidelines on prevention and management." J Feline Med Surg **11**(7): 556-564.

Radford, A. D., K. P. Coyne, S. Dawson, C. J. Porter and R. M. Gaskell (2007). "Feline calicivirus." Vet Res **38**(2): 319-335.

Radford, A. D., S. Dawson, K. P. Coyne, C. J. Porter and R. M. Gaskell (2006). "The challenge for the next generation of feline calicivirus vaccines." Vet Microbiol **117**(1): 14-18.

Radford, A. D., S. Dawson, R. Ryvar, K. Coyne, D. R. Johnson, M. B. Cox, E. F. Acke, D. D. Addie and R. M. Gaskell (2003). "High genetic diversity of the immunodominant region of the feline calicivirus capsid gene in endemically infected cat colonies." Virus Genes **27**(2): 145-155.

Radford, A. D., P. C. Turner, M. Bennett, F. McArdle, S. Dawson, M. A. Glenn, R. A. Williams and R. M. Gaskell (1998). "Quasispecies evolution of a hypervariable region of the feline calicivirus capsid gene in cell culture and in persistently infected cats." J Gen Virol **79 (Pt 1)**: 1-10.

Radford, A. D., K. Willoughby, S. Dawson, C. McCracken and R. M. Gaskell (1999). "The capsid gene of feline calicivirus contains linear B-cell epitopes in both variable and conserved regions." J Virol **73**(10): 8496-8502.

Reynolds, B. S., H. Poulet, J.-L. Pingret, D. Jas, S. Brunet, C. Lemeter, M. Etievant and C. Boucraut-Baralon (2009). "A nosocomial outbreak of feline calicivirus associated virulent systemic disease in France." J Feline Med Surg **11**(8): 633-644.

Rohayem, J., I. Robel, K. Jager, U. Scheffler and W. Rudolph (2006). "Protein-primed and de novo initiation of RNA synthesis by norovirus 3Dpol." J Virol **80**(14): 7060-7069.

Ruch-Gallie, R. A., J. K. Veir, J. R. Hawley and M. R. Lappin (2011). "Results of molecular diagnostic assays targeting feline herpesvirus-1 and feline calicivirus in adult cats administered modified live vaccines." J Feline Med Surg **13**(8): 541-545.

Rust, R. C., L. Landmann, R. Gosert, B. L. Tang, W. Hong, H. P. Hauri, D. Egger and K. Bienz (2001). "Cellular COPII proteins are involved in production of the vesicles that form the poliovirus replication complex." J Virol **75**(20): 9808-9818.

Rybak, S. L. and R. F. Murphy (1998). "Primary cell cultures from murine kidney and heart differ in endosomal pH." J Cell Physiol **176**(1): 216-222.

Schaffer, F. L., D. W. Ehresmann, M. K. Fretz and M. I. Soergel (1980). "A protein, VPg, covalently linked to 36S calicivirus RNA." J Gen Virol **47**(1): 215-220.

Schlegel, A., T. H. Giddings, Jr., M. S. Ladinsky and K. Kirkegaard (1996). "Cellular origin and ultrastructure of membranes induced during poliovirus infection." J Virol **70**(10): 6576-6588.

Schorr-Evans, E. M., A. Poland, W. E. Johnson and N. C. Pedersen (2003). "An epizootic of highly virulent feline calicivirus disease in a hospital setting in New England." J Feline Med Surg **5**(4): 217-226.

Seal, B. S. (1994). "Analysis of capsid protein gene variation among divergent isolates of feline calicivirus." Virus Res **33**(1): 39-53.

Seal, B. S., J. F. Ridpath and W. L. Mengeling (1993). "Analysis of feline calicivirus capsid protein genes: identification of variable antigenic determinant regions of the protein." J Gen Virol **74 (Pt 11)**: 2519-2524.

SJ, L., X. HP, P. BQ and Q. NH (1984). "A new viral disease in rabbits." Anim. Husb. Vet. Med. **16**: 3.

Smith, A. W., T. G. Akers, S. H. Madin and N. A. Vedros (1973). "San Miguel sea lion virus isolation, preliminary characterization and relationship to vesicular exanthema of swine virus." Nature **244**(5411): 108-110.

Smith, A. W., D. E. Skilling, N. Cherry, J. H. Mead and D. O. Matson (1998). "Calicivirus emergence from ocean reservoirs: zoonotic and interspecies movements." Emerg Infect Dis **4**(1): 13-20.

Sorkin, A. (2000). "The endocytosis machinery." J Cell Sci **113 Pt 24**: 4375-4376.

Sosnovtsev, S. and K. Y. Green (1995). "RNA transcripts derived from a cloned full-length copy of the feline calicivirus genome do not require VpG for infectivity." Virology **210**(2): 383-390.

Sosnovtsev, S. V., G. Belliot, K. O. Chang, O. Onwudiwe and K. Y. Green (2005). "Feline calicivirus VP2 is essential for the production of infectious virions." J Virol **79**(7): 4012-4024.

Sosnovtsev, S. V., M. Garfield and K. Y. Green (2002). "Processing map and essential cleavage sites of the nonstructural polyprotein encoded by ORF1 of the feline calicivirus genome." J Virol **76**(14): 7060-7072.

Sosnovtsev, S. V., E. A. Prikhod'ko, G. Belliot, J. I. Cohen and K. Y. Green (2003). "Feline calicivirus replication induces apoptosis in cultured cells." Virus Research **94**(1): 1-10.

Sosnovtsev, S. V., S. A. Sosnovtseva and K. Y. Green (1998). "Cleavage of the feline calicivirus capsid precursor is mediated by a virus-encoded proteinase." J Virol **72**(4): 3051-3059.

Sosnovtseva, S. A., S. V. Sosnovtsev and K. Y. Green (1999). "Mapping of the feline calicivirus proteinase responsible for autocatalytic processing of the nonstructural polyprotein and identification of a stable proteinase-polymerase precursor protein." J Virol **73**(8): 6626-6633.

Steinhauer, D. A., E. Domingo and J. J. Holland (1992). "Lack of evidence for proofreading mechanisms associated with an RNA virus polymerase." Gene **122**(2): 281-288.

Stuart, A. D. and T. D. Brown (2006). "Entry of feline calicivirus is dependent on clathrin-mediated endocytosis and acidification in endosomes." J Virol **80**(15): 7500-7509.

Stuart, A. D. and T. D. Brown (2007). "Alpha2,6-linked sialic acid acts as a receptor for Feline calicivirus." J Gen Virol **88**(Pt 1): 177-186.

Studdert, M. J. and J. D. O'Shea (1975). "Ultrastructural studies of the development of feline calicivirus in a feline embryo cell line." Arch Virol **48**(4): 317-325.

Sykes, J. E., V. P. Studdert and G. F. Browning (1998). "Detection and strain differentiation of feline calicivirus in conjunctival swabs by RT-PCR of the hypervariable region of the capsid protein gene." Arch Virol **143**(7): 1321-1334.

Taira, O., M. Suzuki, Y. Takeuchi, Y. Aramaki, I. Sakurai, T. Watanabe, K. Motokawa, S. Arai, H. Sato and N. Maehara (2005). "Expression of feline interferon-alpha subtypes in Esherichia coli, and their antiviral activity and animal species specificity." J Vet Med Sci **67**(5): 543-545.

Tohya, Y., Y. Taniguchi, E. Takahashi, E. Utagawa, N. Takeda, K. Miyamura, S. Yamazaki and T. Mikami (1991). "Sequence analysis of the 3'-end of feline calicivirus genome." Virology **183**(2): 810-814.

Topping, J. R., H. Schnerr, J. Haines, M. Scott, M. J. Carter, M. M. Willcocks, K. Bellamy, D. W. Brown, J. J. Gray, C. I. Gallimore and A. I. Knight (2009). "Temperature inactivation of Feline calicivirus vaccine strain FCV F-9 in comparison with human noroviruses using an RNA exposure assay and reverse transcribed quantitative real-time polymerase chain reaction-A novel method for predicting virus infectivity." J Virol Methods **156**(1-2): 89-95.

Towner, J. S., T. V. Ho and B. L. Semler (1996). "Determinants of membrane association for poliovirus protein 3AB." J Biol Chem **271**(43): 26810-26818.

Tsai, B. (2007). "Penetration of nonenveloped viruses into the cytoplasm." Annu Rev Cell Dev Biol **23**: 23-43.

van Heel, M., G. Harauz, E. V. Orlova, R. Schmidt and M. Schatz (1996). "A new generation of the IMAGIC image processing system." J Struct Biol **116**(1): 17-24.

Vashist, S., D. Bailey, A. Putics and I. Goodfellow (2009). "Model systems for the study of human norovirus Biology." Future Virology **4**(4): 12.

Victoria, M., M. P. Miagostovich, M. S. Ferreira, C. B. Vieira, J. M. Fioretti, J. P. Leite, R. Colina and J. Cristina (2009). "Bayesian coalescent inference reveals high evolutionary rates and expansion of Norovirus populations." Infect Genet Evol **9**(5): 927-932.

Wang, Q. H., M. G. Han, S. Cheetham, M. Souza, J. A. Funk and L. J. Saif (2005). "Porcine noroviruses related to human noroviruses." Emerg Infect Dis **11**(12): 1874-1881.

Wei, L., J. S. Huhn, A. Mory, H. B. Pathak, S. V. Sosnovtsev, K. Y. Green and C. E. Cameron (2001). "Proteinase-polymerase precursor as the active form of feline calicivirus RNA-dependent RNA polymerase." J Virol **75**(3): 1211-1219.

White, S. D., R. A. Rosychuk, T. A. Janik, P. Denerolle and P. Schultheiss (1992). "Plasma cell stomatitis-pharyngitis in cats: 40 cases (1973-1991)." J Am Vet Med Assoc **200**(9): 1377-1380.

WHO (2009). "World Health Organization: Diarrhoeal Diseases (Updated February 2009)." [http://www.who.int/vaccine_research/diseases/diarrhoeal/en/index.html].

Willcocks, M. M., M. J. Carter and L. O. Roberts (2004). "Cleavage of eukaryotic initiation factor eIF4G and inhibition of host-cell protein synthesis during feline calicivirus infection." J Gen Virol **85**(Pt 5): 1125-1130.

Wirblich, C., G. Meyers, V. F. Ohlinger, L. Capucci, U. Eskens, B. Haas and H. J. Thiel (1994). "European brown hare syndrome virus: relationship to rabbit hemorrhagic disease virus and other caliciviruses." J Virol **68**(8): 5164-5173.

Wobus, C. E., S. M. Karst, L. B. Thackray, K.-O. Chang, S. V. Sosnovtsev, G. l. Belliot, A. Krug, J. M. Mackenzie, K. Y. Green and H. W. Virgin (2004). "Replication of Norovirus in Cell Culture Reveals a Tropism for Dendritic Cells and Macrophages." PLoS Biology **2**(12): 9.

Wobus, C. E., L. B. Thackray and H. W. V. IV (2006). "Murine Norovirus: a Model System To Study Norovirus Biology and Pathogenesis." J Virol **80**(11): 10.

Woode, G. N. and J. C. Bridger (1978). "Isolation of small viruses resembling astroviruses and caliciviruses from acute enteritis of calves." J Med Microbiol **11**(4): 441-452.

Wu, J., G. Zheng and L. M. Lee (2012). "Optical imaging techniques in microfluidics and their applications." Lab Chip **12**(19): 3566-3575.

Zhou, Z. H., S. Hardt, B. Wang, M. B. Sherman, J. Jakana and W. Chiu (1996). "CTF determination of images of ice-embedded single particles using a graphics interface." J Struct Biol **116**(1): 216-222.

Zwillenberg, L. O. and F. Burki (1966). "On the capsid structure of some small feline and bovine RNA viruses." Arch Gesamte Virusforsch **19**(4): 373-384.